T.R.
EGE UNIVERSITY
Graduate School of Applied and Natural
Science

APPLICATION OF REVERSE ELECTRODIALYSIS METHOD FOR SALINITY GRADIENT ENERGY GENERATION

Orhan KINALI

Supervisor : Prof. Dr. Nalan KABAY
Co-advisor : Dr. Enver GÜLER

Chemical Engineering Department
Chemical Engineering Second Cycle Programme

İzmir
2021

EGE ÜNİVERSİTESİ FEN BİLİMLERİ ENSTİTÜSÜ

ETİK KURALLARA UYGUNLUK BEYANI

EÜ Lisansüstü Eğitim ve Öğretim Yönetmeliğinin ilgili hükümleri uyarınca Yüksek Lisans Tezi olarak sunduğum "APPLICATION OF REVERSE ELECTRODIALYSIS METHOD FOR SALINITY GRADIENT ENERGY GENERATION" başlıklı bu tezin kendi çalışmam olduğunu, sunduğum tüm sonuç, döküman, bilgi ve belgeleri bizzat ve bu tez çalışması kapsamında elde ettiğimi, bu tez çalışmasıyla elde edilmeyen bütün bilgi ve yorumlara atıf yaptığımı ve bunları kaynaklar listesinde usulüne uygun olarak verdiğimi, tez çalışması ve yazımı sırasında patent ve telif haklarını ihlal edici bir davranışımın olmadığını, bu tezin herhangi bir bölümünü bu üniversite veya diğer bir üniversitede başka bir tez çalışması içinde sunmadığımı, bu tezin planlanmasından yazımına kadar bütün safhalarda bilimsel etik kurallarına uygun olarak davrandığımı ve aksinin ortaya çıkması durumunda her türlü yasal sonucu kabul edeceğimi beyan ederim.

25 / 08 / 2021

Orhan KINALI

ÖZET

Tuzluluk Farkından Enerji Üretimi İçin Ters Elektrodiyaliz Yönteminin Uygulanması

KINALI, Orhan
Yüksek Lisans Tezi, Kimya Mühendisliği Bölümü
Tez Danışmanı: Prof. Dr. Nalan KABAY
İkinci Danışman: Dr. Enver GÜLER
Ağustos 2021, 49 sayfa

Bu tez çalışmasında çevre dostu, temiz enerji üretimine yönelik, farklı tuz derişimlerine sahip su akımlarının oluşturduğu tuzluluk farkından (gradyanından) yararlanarak ters elektrodiyaliz (RED) yönteminin uygulanmasına yönelik performans analizleri yapılmıştır.

Çalışmalarda, sisteme beslenen tuzlu su (NaCl) çözeltileri kullanılmıştır. Performans analizlerinde farklı hücre çifti konfigürasyonları (3, 5, 7 ve 10 çift), farklı tuzluluk gradyanları (1:30, 2:30 ve 1:45) ve farklı çizgisel akış hızları (0.208 cm/s, 0.417 cm/s, 0.625 cm/s, 0.833 cm/s) incelenmiştir. Performans analizleri potansiyostat cihazı aracılığıyla yapılmıştır. Elde edilebilecek maksimum güç ve güç yoğunluğu değerleri hesaplanmış, açık devre voltaj (OCV) değerleri incelenmiştir.

Çalışma sonucunda tuzluluk gradyan enerjisi üretiminde ters elektrodiyaliz yönteminin başarıyla uygulanabileceği anlaşılmıştır. Optimum besleme akış hızında farklı tuz oranları incelendiğinde 1:30, 2:30 ve 1:45 tuz oranlarında sırasıyla 0.280, 0.210 ve 0.352 W/m^2 elektriksel güç yoğunlukları elde edilmiştir. Elde edilen en yüksek OCV değeri 10 çift membran için 1.414 V olarak tespit edilmiştir. İncelenen parametrelere göre, tuzluluk gradyanındaki, hücre çifti sayısı ve besleme akış hızlarındaki artışın; üretilen güçte, güç yoğunluğunda ve OCV üzerinde de artış sağladığı tespit edilmiştir.

Anahtar Kelimeler: Ters elektrodiyaliz (RED), tuzluluk gradyanı enerjisi, enerji üretimi, iyon değiştirici membran

ABSTRACT

Application of Reverse Electrodialysis Method For Salinity Gradient Energy Generation

KINALI, Orhan

Master Science Thesis, Chemical Engineering Department

Supervisor: Prof. Dr. Nalan KABAY

Co-advisor: Dr. Enver GÜLER

August 2021, 49 pages

In this thesis, performance analyzes have been done for the application of the reverse electrodialysis (RED) method by utilizing the salinity difference (gradient) created by the water streams with different salt concentrations for environmentally friendly, clean energy production.

The system has been simulated with artificial salt water (NaCl) feeds, pumped with peristaltic pumps. In the performance analyses, different membrane pairs configurations (3, 5, 7 and 10 pairs), different salinity gradients (1:30, 2:30 and 1:45) and different linear flow rates (0.208 cm/s, 0.417 cm/s, 0.625 cm/s, and 0.833 cm/s) are investigated. The performance analyses were obtained with the help of a potentiostat. Maximum obtainable power and power density values are calculated. Open circuit voltage values were examined.

The study revealed that, the reverse electrodialysis method has been applied successfully in the generation of salinity gradient energy. When the different salt ratios were examined at optimum feed linear flow rates, electrical power densities of 0.280, 0.210 and 0.352 W/m^2 were obtained from 1:30, 2:30 and 1:45 salt ratios, respectively. Highest OCV value obtained was 1.414 V for 10 pairs of membranes. According to the examined parameters, it is revealed that with the increase in salinity gradient, the number of membrane pairs and feed flow rates; power generated, power density and OCV increases.

Keywords: Reverse electrodialysis (RED), salinity gradient energy, energy generation, ion exchange membrane

To my family…

TABLE OF CONTENTS

Page

LIST OF FIGURES

LIST OF FIGURES (Continued)

LIST OF FIGURES (Continued)

Figure Page

LIST OF TABLES

LIST OF TABLES (Continued)

NOMENCLATURE

AEM	Anion exchange membrane
CEM	Cation exchange membrane
HCC	High concentrate compartment
IEM	Ion exchange membrane
LCC	Low concentrate compartment
OCV	Open circuit voltage
RED	Reverse electrodialysis
SGE	Salinity gradient energy
W	Power (W)
P	Power (W)
P	Power density (W/m2)
V	Potential (V)
I	Current (A)
A	Area (m^2)
Δ	Difference
α	Selectivity
N	Number of membrane pairs
R	Gas constant (8.314 J/mol.K)

NOMENCLATURE (Continued)

T	Temperature (K)
z	Ion charge
F	Faraday constant (96485 C/mol)
a	Concentration (mol/L)
R	Resistance (Ω)
R	Resistance (Ω)
d	Thickness (m)
K	Conductivity (S/m)
ε	Electromotive force (V)

1. INTRODUCTION

1.1. Salinity Gradient Energy (SGE)

Renewable energy sources are widely listed as wind, solar, geothermal, hydroelectricity. The demand to reduce the fossil fuel consumption, and the CO_2 emissions, points the direction into renewable energy sources (Micale et al., 2016). The advance in technology heading the energy consumption to renewable sources, day by day new sustainable energy sources are taking a share in the energy market.

Salinity gradient energy (SGE) which was originated from osmotic energy is a lesser known source with a high potential. It was firstly explained in 1954 by R.E. Pattle (Pattle, 1954). Simply, this valuable energy source involves of controlled mixing water streams with different salinity levels (Mei and Tang, 2018).

The process of mixing two different water streams with different salinity levels results in a spontaneous energy release (Cipollina and Micale, 2016, Rijnaarts, 2018). SGE, releases as a chemical potential energy, acquired by mixing two different water streams with different salinity levels, given as river water and seawater. It is defined as sustainable, completely clean energy source with no release of CO_2 and other toxic fumes/gases to the environment (Jones and Finley, 2003, Tufa et al., 2018).

Worldwide the intersection point of where the rivers discharged into the ocean, the theoretical energy that can be generated via salinity gradient energy level is 1.4-2.6 TW (Pawlowski, 2015). According to Kuleszo, this theoretical potential stated as 1.724 TW and the technical potential is stated as 0.983 TW which if obtainable from 5472 rivers worldwide known (Table 1.1). Technical potential is the 57% of total theoretical potential (Kuleszo et al., 2010). Alvarez-Silva et al. (2016) states as 625 TWh/yr of SGE is shown to be possible when river streams are technically utilized. According to Skråmestø et al. (2009), researchers reported that an estimation of 1650 TWh/yr is viable for SGE generation.

Table 1.1. Theoretical and technical potentials of salinity gradient power by world region (Kuleszo et al., 2010).

Region	Number of Rivers	Discharge	Theoretical Potential		Technical Potential		
			GW	%	GW	%	As % of theoretical
Africa	391	170,294	311	18	190	19	61
Asia	1243	236,769	374	22	206	21	55
Australia	251	15,818	30	2	20	2	65
Europe	779	74,569	94	5	56	6	59
North America	1878	191,434	321	19	189	19	59
Oceania	540	149,748	278	16	175	18	63
South America	390	320,078	316	18	148	15	47
World	5472	1,158,709	1,724	100	983	100	57

Worldwide salinity gradient energy capacity is calculated as more than 27,000 TWh/yr with taking consideration of known water sources as reference. The obtainable value is around 2000 TWh/yr, resulting this energy source potential to be more than 10% of total renewable energy sources (Post el al., 2008) pointing that this potential is valuable and should not be ignored.

The aim of this thesis is to use reverse electrodialysis (RED) method for generation of environmentally friendly, clean energy via using water streams with different salt concentrations and their performance analyses. In the performance analyses, different membrane pair configurations (3, 5, 7 and 10 pairs), different salinity gradients (1:30, 2:30 and 1:45) and different linear flow rates (0.208 cm/s, 0.417 cm/s, 0.625 cm/s, 0.833 cm/s) are investigated.

1.2. Methods for SGE Generation

Salinity gradient energy can be generated by different technologies:
Reverse electrodialysis (RED), microbial RED, pressure retarded osmosis (PRO), capacitive mixing (CAPMIX), vapor pressure difference utilization (VPD), and mixing entropy batteries (MEB). RED and PRO are the most applicable and result oriented membrane-based technologies which are at the most advanced stage of development (Tufa et al., 2018).

PRO systems are in need of more concentrated salt water while RED systems are applicable with the river water and seawater as feed streams pointing that the RED systems require more advanced technological setup (Guler, 2014). PRO systems works by the water flow under osmotic pressure thus energy is generated via the movement of turbines, in the RED system, energy is generated by electrochemical process (Bharadwaj et al., 2016). Both processes are separation methods with membranes and are based on osmotic power (Fouad, 2016).

1.3. Reverse Electrodialysis (RED)

The driving force of system is the chemical potential difference in between both solutions (river water and seawater) for RED process. The driving force generates a voltage over each membrane, and the overall potential of the system is the sum of the potential differences over membranes.

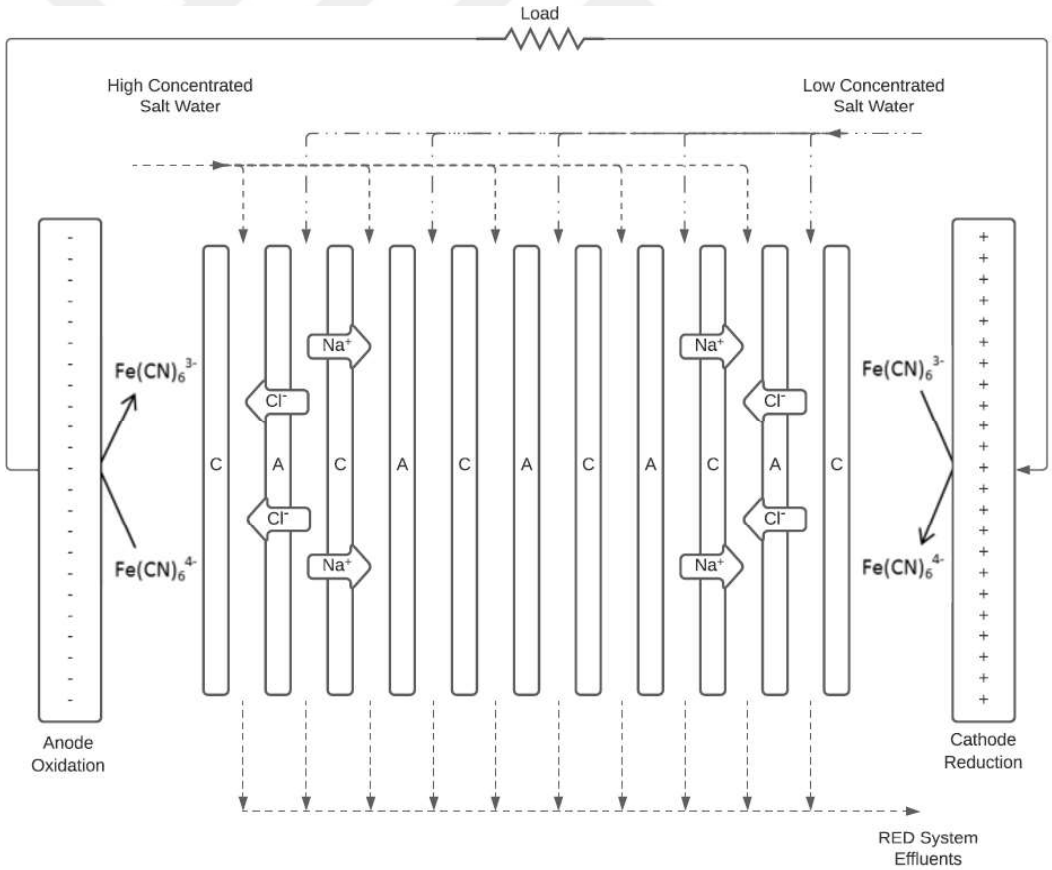

Figure 1.1. Schematic representation of RED principle

This result generates an ionic flux, which is then converted into electricity by a redox reaction occurring at the electrodes connected to an external circuit.

In RED, two contiguous ion exchange membranes, gets together to create a single cell pair, consisting of an anion exchange membrane, a low concentrate compartment, a cation exchange membrane and a high concentrate compartment (Figure 1.1.).

SGE produced by RED system is affected by operational parameters such as salinity difference, flow rate, temperature, residence time, the number of cell pairs in the stack, membrane and spacer characteristics (Ortiz-Imedio et al., 2019).

Overall information (project name, location, properties, project consortium, start-up dates) on RED pilot plants reported in the literature is given in Table 1.2.

Table 1.2. Overall information on RED pilot plants (Cipollina and Micale, 2016).

Project	Plant Location	Feed Solutions	Project Consortium	Plant Start-Up
Blue Energy	Afsluitdijk (The Netherlands)	Seawater (≈28 g/L) and river water or lake water (≈0.2-0.5 g/L)	REDstack (NL), Wetsus (NL), A. Hak (NL), Alliander (NL), Fujifilm (NL), Magneto Special Anodes (NL)	November 2014
REAPower	Marsala (Italy)	Saltworks brine (200-300 g/L) and brackish water (2-3 g/L)	WIP (DE), VITO (BE), University of Palermo (IT), Fujifilm (NL), REDstack (NL), Kraton (NL), SolarSpring (DE), Next Technology Tecnotessile (IT), UNIMAN (UK), University of Calabria (IT), DNV-GL (NL)	March 2014

1.4. Challenges in Reverse Electrodialysis (RED) Process

1.4.1. Pumping of feed streams

Salt water streams which are used as feed streams need to be pumped into the stack and leave the system. While making this process work, an important topic needs to be pointed, which is large volume needs to be fed into the system. Considering the main goal of this process, which is to generate energy, process optimization is required. While designing the process, using the nature elements is a big opportunity. The water flowing with its own charm, using the potential of already flowing water sources is another good point of design, thus reducing the power consumption of pumping.

In addition, environmental legislation for the preservation of nature is another important point. The pumping of large volumes of water can create sheer forces that are enough to harm certain animal or plant species (Schaetzle and Buisman, 2015).

1.4.2. Filtration of feed streams

Filtration of pumped water with living creatures, such as fishes in the pumped water, and stones or large particles may block the streams. Filtering can be step-designed from coarse to fine. Big drum filters can separate solid particles from the solutions to different mesh filters. In the optimization of this step, great emphasis needs to be placed on the trade-off between the filtration efficiency and the energy requirement for filtration (Schaetzle and Buisman, 2015).

1.4.3. Internal resistance of RED stack

Since the process is an electrochemical system, the internal resistance must be kept as low as possible. In order to achieve this goal, the space between each membrane should be kept small in the micrometer dimension. In the general design, between membranes; spacers and gasket items are placed. Placing these items creates dead zones inside of the stack between two membranes, decreasing the performance (Schaetzle and Buisman, 2015). This effect also can be explained as, spacers and gaskets placed on membranes, resulting with covering membrane area, and resisting the ions to pass through membranes.

1.4.4. Multivalent ions in the feed streams

In the literature, researchers observed that the presence of only a small concentration of divalent cations, such as Ca^{2+} or Mg^{2+}, can significantly decrease the power output of the system (29%–50% lower power densities for a 10% molar fraction of Mg^{2+} salts) (Vermaas et al., 2014).

1.4.5. Substances, chemicals, biofouling agents that may damage membranes

Feeding streams directly from nature results with water having traces of different chemicals, substances and biofouling agents; such as charged species like humic acids or negatively charged clay particles, or bacteria population which can accumulate on the surface of the membranes and damage over time (Rijnaarts et al., 2019).

2. GENERAL INFORMATION

2.1. Introduction

Figure 2.1 shows an important component in reverse electrodialysis (RED) system, the membrane stack (module).

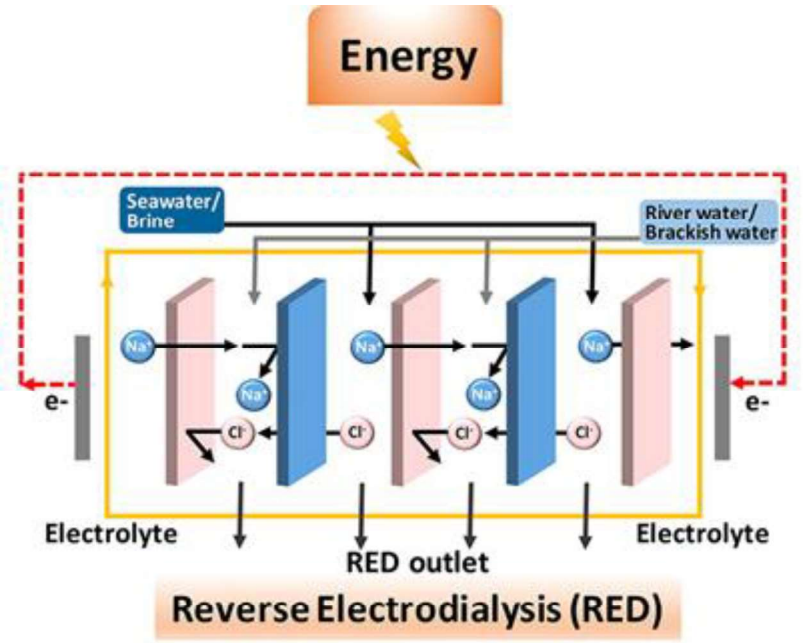

Figure 2.1. Reverse electrodialysis (RED) system (Tufa et al., 2018).

In the RED system, cation exchange (CEM) and anion exchange (AEM) membranes are placed side by side to create the membrane module. Membrane module is created by placing high concentrated salt compartments and low concentrated salt compartments side by side to form a series, and are fed with solutions having high salt concentration and low salt concentration. The salinity difference and the charge transport occured at the ion exchange membranes generates an electrochemical potential (Hong et al., 2019).

The hydrodynamic resistance and overall stack resistance are highly affected by the flow rates of solutions in RED system. Hydrodynamic resistance affects overall internal stack resistance and it should be minimized for maximum open circuit voltage (OCV). At low flow rates, concentration polarization causes higher internal resistance and lower concentration gradient. On the other hand, at higher flow rates, less internal resistance and higher OCV levels are observed (Gilstrap, 2013).

The ion flux formed is converted into electrical energy by redox reactions taking place at the electrodes by creating an external circuit current. Electrode selection is adjusted by selecting suitable electrode materials and appropriate electrode rinse solutions. In the RED systems, two contiguous ion exchange membranes (IEM) form a single cell element (also named as cell pair). This cell element includes an anion exchange membrane (AEM), a low concentrated salt compartment (i.e., river water), a cation exchange membrane (CEM) and a high concentrated salt compartment (i.e., seawater). The electrode system required for the RED unit set up by two electrodes (anode and cathode) placed in the outer part of the system and an electrode rinse solution containing a redox couple suitable for electrochemical reactions (Guler, 2014).

Ions present in the seawater compartment cross selectively through opposing ion exchange membranes (IEMs): anions cross the AEM from the seawater to the river water, while cations pass the CEM from the seawater to the river water, thereby generating a potential across the membranes, known as the Donnan potential (Ohshima and Ohki, 1985, Simões et al., 2021).

2.1.1. Electrode and electrode rinse solutions

According to literature survey, Cipollina and Micale summarized the electrodes and electrode rinse solutions in Figure 2.2 (Cipollina and Micale, 2016).

Veerman et al. investigated suitable electrode systems for RED, compared a number of electrode systems regarding technical feasibility, and economically, considering health and safety. The evaluation shows that, the most suitable system proposed was the use of Fe^{2+}/ Fe^{3+} couple in a NaCl-HCl supporting electrode, with Ru/Ir covered titanium electrodes (Veerman et al., 2010). Hexacyanoferrate $[Fe(CN)6]^{4-}$/$[Fe(CN)6]^{3-}$ couple is widely used as redox species in RED systems (Tufa et al., 2018).

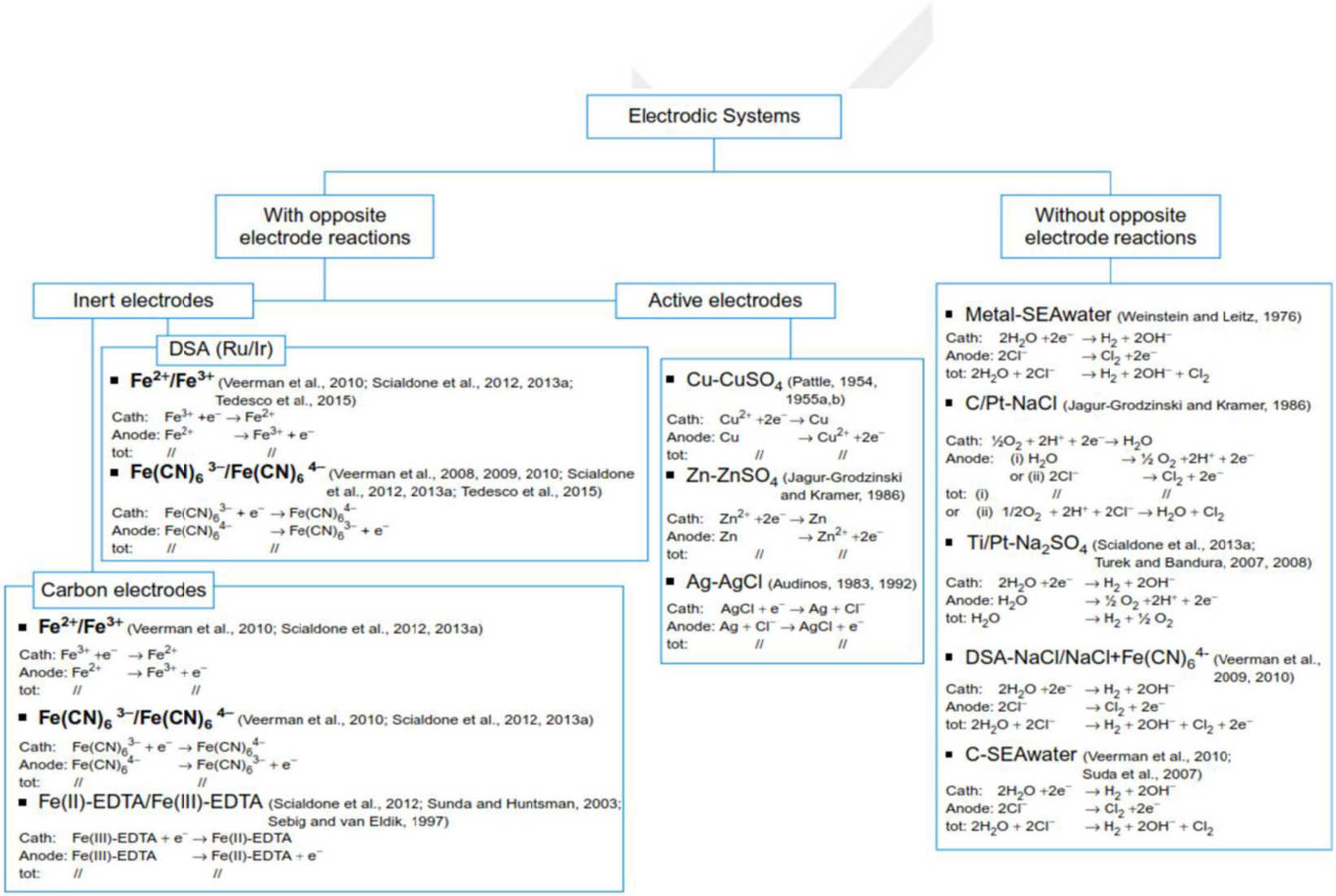

Figure 2.2. Electrode and electrode rinse solutions (Cipollina and Micale, 2016).

2.2. Theoretical Calculations

Open circuit voltage (OCV) and current-voltage analyzes are carried out by chronopotentiometric method. The values obtained are used in the power (P) calculation. The voltage value calculated at zero current value gives the highest voltage value, in other words it is called "open circuit voltage". The highest power density in the studied current density ranges (0-10 A/m^2) is also examined. Chronopotentiometric measurements are taken for 30 seconds at each current value.

Electromotive force (ε) (also called as open circuit voltage), equals to internal resistance (r) multiplied by current (I) with the sum of resistance of other compotents in the circuit (R) multiplied by current (I):

$$\varepsilon = rI + RI \tag{1}$$

Electromotive force is defined as the potential difference of a source of electricity when no current is flowing, which is measured in volts. Internal resistance is the amount of resistance within the voltage source.

The voltage (V) depends on the electromotive force (ε), the internal resistance (r) and the current (I):

$$V = \varepsilon - rI \tag{2}$$

The produced electrical power (Watt) is found by multiplying each current (I) and the corresponding potential difference (V). Power density is defined as the power generated per membrane area (A). These values are also calculated by Equation 4.

$$W = V \cdot I \tag{3}$$

$$P = \frac{W}{2AN} \tag{4}$$

In this equation, P is the power density (W/m^2), W is the electrical power (W), A is the active membrane area (m^2) and N is the number of membranes.

A potential difference (ΔV^o) or called "Open Circuit Voltage - E_{OCV}" occurs between the two sides of a membrane due to ion transport. This theoretical potential difference is calculated by the Nernst equation for monovalent salt solutions (e.g. NaCl solutions) (Jagur-Grodzinskr, 1986, Lacey, 1980):

$$\Delta V^o = E_{OCV} = N\frac{2\alpha RT}{zF}\ln\left(\frac{a_c}{a_d}\right) \quad (5)$$

Here, ΔV^o is the potential difference (V) for the theoretical membrane stack, α is the average selectivity of membrane pairs, N is the number of membrane pairs, R is gas constant (8.314 J/mol.K), T is the absolute temperature (K), z is ion charge, F refers to the Faraday constant (96485 C/mol), a_c is the high concentrated salt solution concentration (mol/L) ve a_d is the low concentrated salt solution concentration (mol/L).

In Equation 5, the logarithmic term gives the salt, it is seen that the salt ratio is directly proportional to the potential.

Neglecting the non-ohmic resistances, i.e. the sum of boundary layer resistance (due to concentration polarization) and the resistance due to the change of the concentration of bulk solution, the stack resistance can be defined as (Długołecki et al., 2008, Weinstein et al., 1976):

$$\mathrm{R_{stack}} = \frac{\mathrm{N}}{\mathrm{A}} \times \left(\mathrm{R_{aem}} + \mathrm{R_{cem}} + \frac{\mathrm{d_c}}{\mathrm{K_c}} + \frac{\mathrm{d}_d}{\mathrm{K_d}}\right) + \mathrm{R_{el}} \quad (6)$$

where A is effective membrane area (m^2), R_{aem} is the anion exchange membrane resistance ($\Omega \cdot m^2$), R_{cem} is the cation exchange membrane resistance ($\Omega\ m^2$), d_c is the thickness of the concentrated saltwater compartment (m), d_d is the thickness of the diluted saltwater compartment (m), K_c is the conductivity in the concentrated saltwater compartment ($S\ m^{-1}$), K_d is the conductivity in the diluted saltwater compartment ($S\ m^{-1}$) and R_{el} is the ohmic resistance of both electrodes and their compartments (Ω).

The maximum power output using R_{stack} and E_{OCV} can subsequently be expressed as (Długołecki et al., 2008, Guler, 2014, Veerman et al., 2008):

$$P_{max} = \frac{(E_{OCV})^2}{4R_{stack}} \quad (7)$$

Then, the maximum power output can be easily extended by substituting E_{OCV} in Equation 7 by Equation 5:

$$P_{max} = \frac{\alpha^2}{R_{stack}} \times \left[\frac{NRT}{zF} \ln\left(\frac{a_c}{a_d}\right)\right]^2 \quad (8)$$

In this equation, gross power density is a function of the square of membrane permselectivity α^2 and stack resistance R_{stack}.

Consequently, the power density (power output per unit membrane area, P_{gross}) can be calculated from P_{max}:

$$P_{gross} = \frac{P_{max}}{2AN} \quad (9)$$

where P_{gross} is the maximum gross power density (W m^{-2}), P_{max} is maximum power output (W), A is effective area of single membrane (m^2) and N is the number of membrane cells (-).

2.3. RED Stack

Laboratory scale reverse electrodialysis (RED) system (Figure 2.3) was purchased from STT Products B.V. company (Tolbert, Holland). It has been designed and modified as shown in Figure 2.4, together with peristaltic pumps and solution feed tanks in order to control the system flow rates and to allow operation in desired feed solution volumes.

In the designed process setup, 25 L of feed tanks are present, one for high concentrated salt solution and one for low concentrated salt solution, electrode rinse solution tank (2 L), peristaltic pump (Masterflex) that can transfer both feed solutions to the membrane stack at the same time, for the electrode rinse solution there is a separate peristaltic pump (Masterflex), membrane stack (STT Products BV, Holland). For electrochemical measurements, a potentiostat (Gamry Reference 3000, Gamry, USA) was employed (Figure 2.4). The flow chart of the system is given in Figure 2.5.

Sodium chloride (NaCl) salt (Extra pure, Tekkim Kimya San. Tic. Ltd. Şti.) was used to prepare salt solutions, potassium ferrocyanide ($K_4Fe(CN)_6$) and potassium ferricyanide ($K_3Fe(CN)_6$) salts (Pro analyst, Merck) were used to prepare the electrode rinse solution. All solutions were prepared using deionized water (conductivity: 0.01 mS / cm) obtained from the pure water system in our laboratory.

Figure 2.3. Designed reverse electrodialysis (RED) process, experimental setup

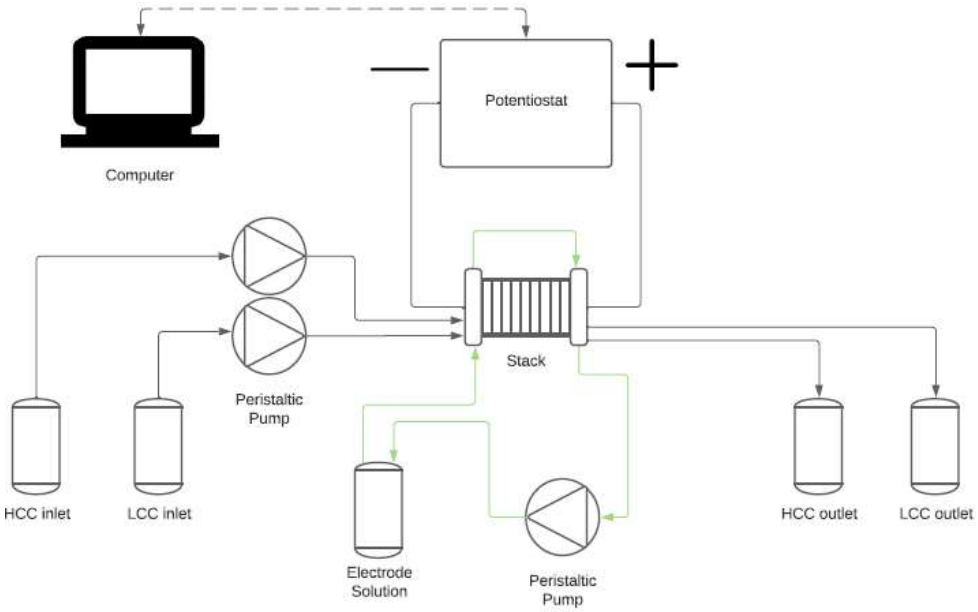

Figure 2.4. Flow diagram regarding the RED system

Table 2.1. The technical information about the RED system

Parameters	*Property*
Active membrane/electrode area	10 x 10 cm
Membrane type	Ralex AMH-PES/CMH-PES
The number of membranes used	3, 5, 7 and 10 membrane pairs
Electrode (anode and cathode)	Ti/Ru-Ir alloy mesh type (mesh 1.0, area: 10x10 cm)
Spacer material / thickness	Polypropylene fabric mesh / 400 μm
Electrode rinse solution flow rate	300 mL/min
Electrode rinse solution	0.05 M $K_4Fe(CN)_6 \cdot 3H_2O$ / 0.05 M $K_3Fe(CN)_6$ and 0.25 M NaCl mixture
Feed water type/conductivity (20.0 °C)	More concentrated: 0.513 M NaCl/47.2 mS/cm, 0.770 M NaCl/66.6 mS/cm; Less concentrated: 0.017 M NaCl/1.8 mS/cm, 0.034 M NaCl/3.6 mS/cm
Feed water volumetric flow rate	50, 100, 150, 200 mL/min
Linear flow rate	0.208, 0.417, 0.625, 0.833 cm/s

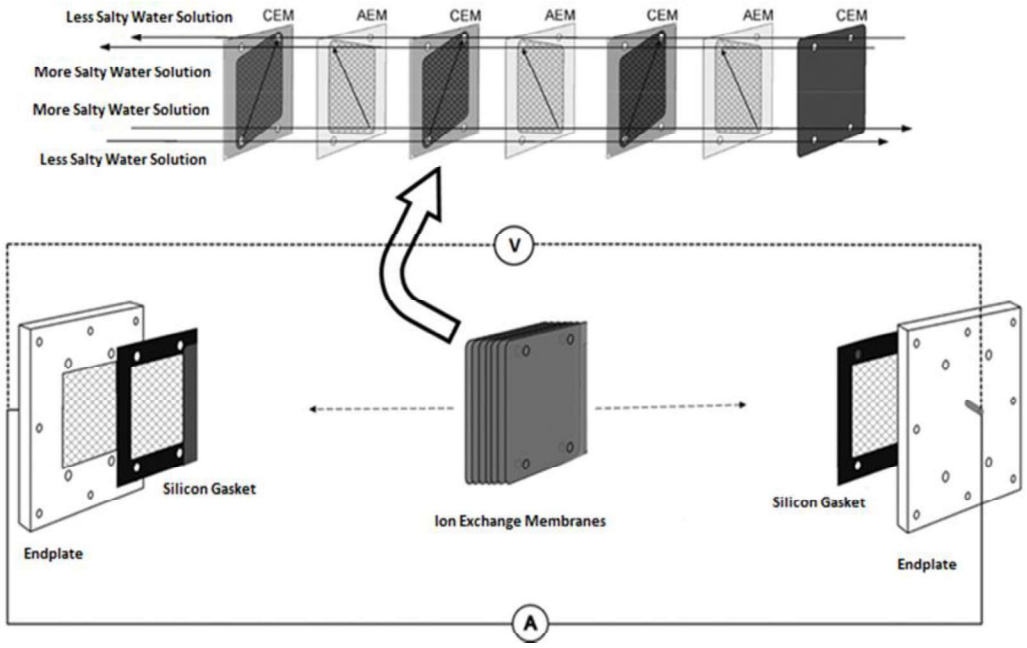

Figure 2.5. Reverse electrodialysis (RED) membrane stack system (Długołęcki et al., 2009)

The RED membrane stack is formed by placing membranes between two end plates with electrodes (Ti-Ru alloy mesh type). Membranes form the membrane stack with cation-anion-cation-anion sequences, respectively (Figure 2.6). An additional cation exchange membrane is placed inside the module to the end, after anion exchange membrane, to prevent the electrode rinse solution (mixture of 0.05 M $K_4Fe(CN)_6 \cdot 3H_2O$, 0.05 M $K_3Fe(CN)_6$ and 0.25 M NaCl) from leaking to the inner membranes. The system is allowed to work with the desired number of membranes. There are polypropylene fabric meshes (spacer) with thickness of 400 micrometers and silicone gaskets between the membranes that will provide liquid passage and sealing. In these studies, 3, 5, 7 and 10 pairs of membranes were placed in the membrane stack. The technical information of the system is given in Table 2.1, and the properties of the membranes used in Table 2.2.

The close-up view of the membranes installed in the RED system is given in Figure 2.7. The membranes used in the system are commercial Ralex brand, which are heterogeneous and relatively thick (≈ 700 μm) membranes, can be seen on Figure 2.8. This thickness increases the electrical resistance of the membranes. The field resistance of these membranes is 7-11 $\Omega.cm^2$ (Table 2.2).

Table 2.2. Technical information about Ralex (MEGA, Czechia) membranes (Guler, 2014)

Membrane	*Film thickness (μm)*	*Area resistance ($\Omega.cm^2$)*	*Permselectivity (%)*	*Swelling degree (%)*	*Ion exchange capacity (meq/g)*	*Charge density (meq/g H_2O)*
CMH-PES	700	11.33	94.7	31.0	2.34	7.6
AMH-PES	714	7.66	89.3	56.0	1.97	3.5

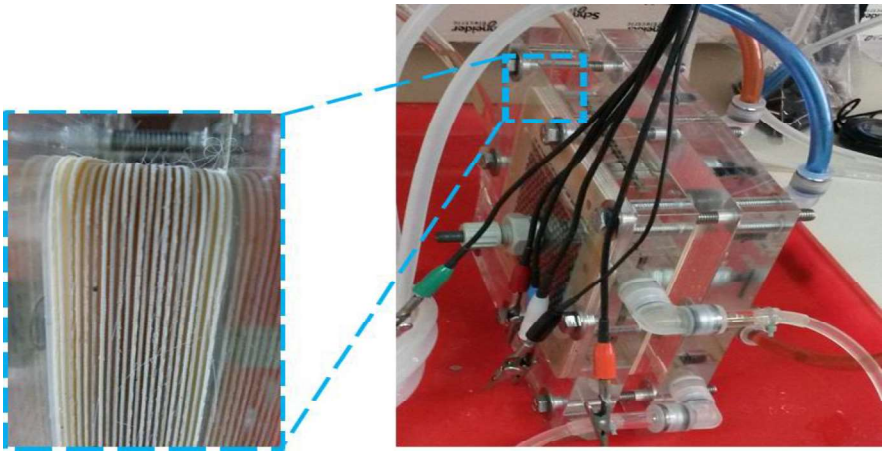

Figure 2.6. The lateral view of the membranes inside the membrane stack

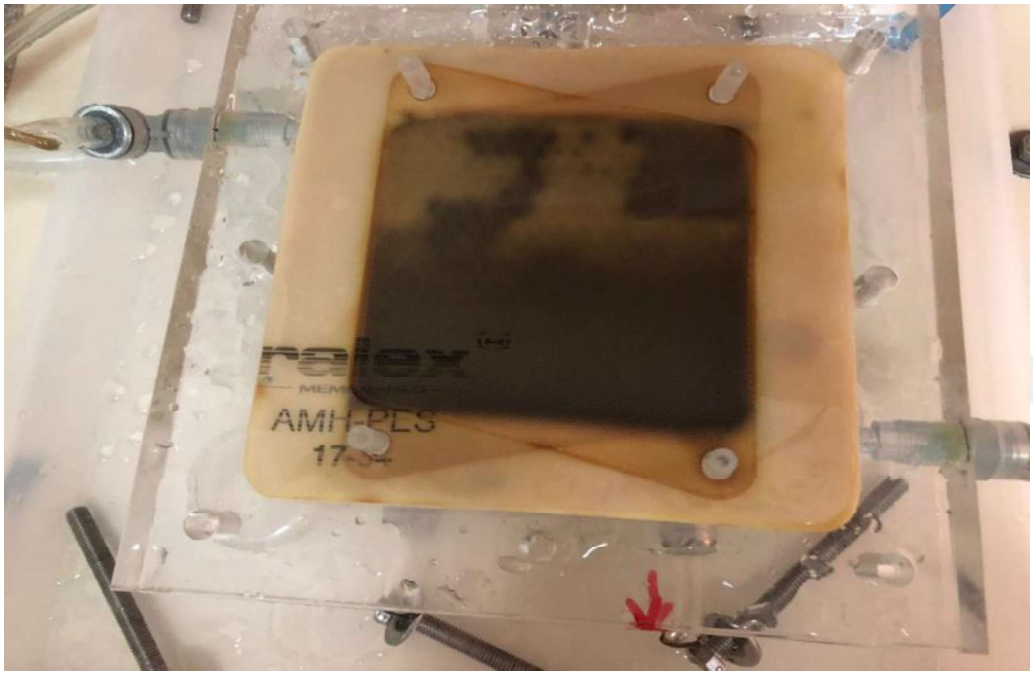

Figure 2.7. The view of Ralex AMH-PES membrane inside the membrane stack

3. EXPERIMENTAL

3.1. Materials

Sodium chloride (NaCl) salt (Extra pure, Tekkim Kimya San. Tic. Ltd. Şti.) was used to prepare salt solutions. Potassium ferrocyanide ($K_4Fe(CN)_6$) and potassium ferricyanide ($K_3Fe(CN)_6$) salts (Pro analyst, Merck) were used to prepare the electrode rinse solution. All solutions were prepared with deionized water (conductivity: 0.01 mS/cm) obtained from the deionized water system in our laboratory.

3.2. Methods

3.2.1. The effects of feed flow rate, salinity gradient, the number of membrane pairs

Feed flow rates applied in RED studies (high concentrated and low concentrated feed salt solutions) were calculated as 0.208, 0.417, 0.625 and 0.833 cm/s, respectively. High concentrated salt solution (30 g and 45 g NaCl/L) and low concentrated salt solution (1 g and 2 g NaCl/L) were used as feed solutions. Salinity and conductivity values were measured with a portable conductivity meter (WTW Cond 3110) (Figure 3.1). The flow rate of the electrode rinse solution is constant and 300 mL/min for all tests. RED tests were conducted in a climated room with temperature-controlled manner at a temperature of 20°C. Heterogeneous RALEX AMH-PES and CMH-PES membranes with 3, 5, 7 and 10 pairs were used in the RED membrane stack. For this purpose, the membrane stack was disassembled and the number of membrane pairs inside was changed.

Figure 3.1. WTW Cond 3110 type conductivity meter.

3.2.2. Performance Analysis

For the performance analysis of the RED system, the GAMRY Reference 3000 Potentiostat/Galvanostat/ZRA model analyzer (Gamry, 2019) was used (Figure 3.2). The device was calibrated before the electrochemical measurements. The cables used in the system were matched to the device and made ready for measurement. Calibration was done with a dummy cell and carried out in a Faraday cage as shown in Figure 3.3. The calibration process should be done when there is any physical intervention on the measuring device (when the system is moved, the power line changes) or if the device gives any message about the calibration of the program. In addition, experimental studies were carried out in an air-conditioned environment (20 °C).

Figure 3.2. Reference 3000 Potentiostat/Galvanostat/ZRA instrumental device

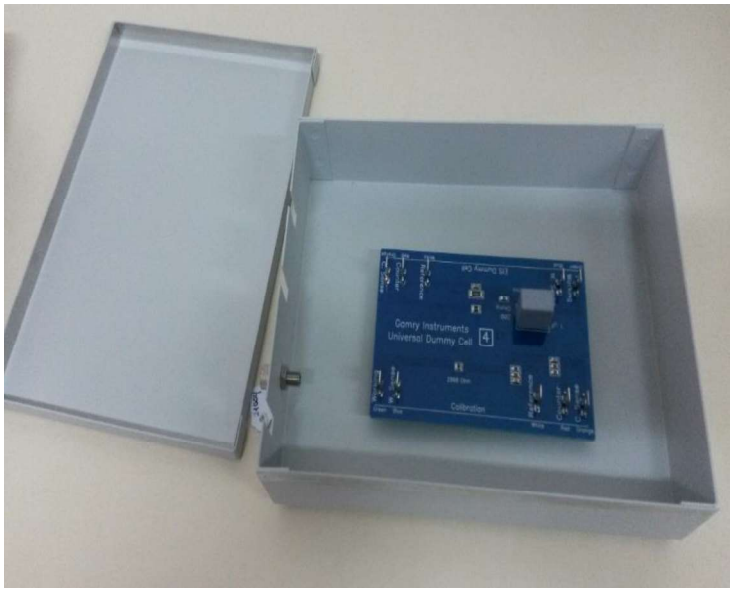

Figure 3.3. Gamry Instruments dummy calibration cell

3.2.3. Blank Tests

In the RED system, in order to prevent the leakage of the electrode rinse solution ($K_4Fe(CN)_6$ and $K_3Fe(CN)_6$ salts) in a closed loop flow, into membranes an extra cation exchange membrane was added to the end of stack, in order, after anion exchange membrane. Thus a blank test was performed to determine gross power. Blank tests were performed in order to calculate the electrical power loss caused by the electrical resistance of this added cation exchange membrane and to determine the power that only the membrane pairs can provide by removing it from the system. First, the membrane stack was removed and the membranes were washed with saturated NaCl solution. Afterwards, a cation exchange membrane was left in the membrane stack, the stack was reassembled and the study was carried out using only a closed circuit electrode rinse solution without using saline solutions. Visuals of the study can be seen in Figures 2.8 and 3.4. Blank test was done before each study. It is also important to do a blank test when a new electrode solution is prepared. Here, in the calculation of the resistance, the results of the study were calculated by subtracting the result obtained by one membrane during blank test from its present state.

A blank test is performed before each run, and it is a process step that must be repeated during any systemical change.

Equation 10 is used to calculate the gross power density.

$$Gross\ Power\ Density\ (W/m^2) = |Power\ Density - Blank\ Power\ Density| \quad (10)$$

In this way, the resistance of the additional cation exchange membrane is calculated and the energy that the system can produce can be calculated in a way that the resistance created in the system is removed. The energy values produced in the system are examined under the effect of the feed flow rate.

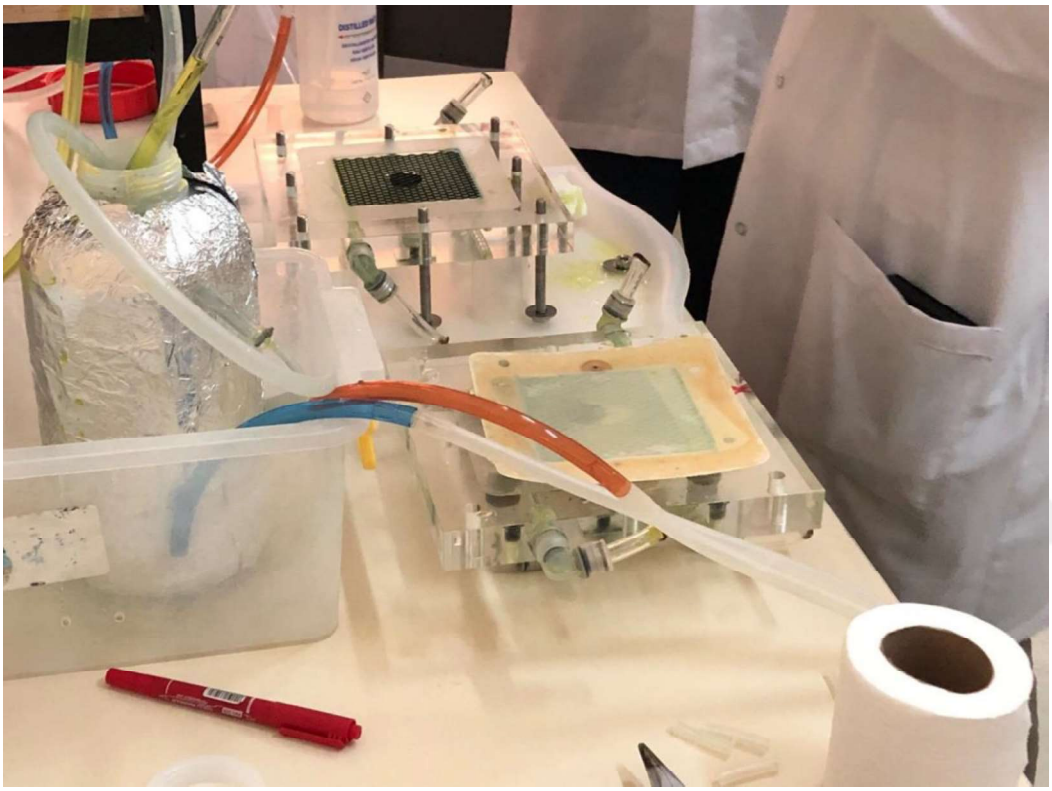

Figure 3.4. Membrane stack dismantling, changing membrane pairs, blank test preparation

3.3. Calculations

Using the experimental data of multiplestep chronopotentiometry (average electrical potential in each step and current value in each step), power generated was calculated by Eq.11. The power density and the current density were calculated from Eqs.12 and 13, respectively. Graphs are plotted according to the current density (A/m^2) and the power density (W/m^2).

$$\text{Power(W)} = \text{Voltage (V)} \times \text{Current (A)} \quad (11)$$

$$\text{Power Density } (W/m^2) = [\text{Power (W)} / \text{Membrane Area}(m^2)] \quad (12)$$

$$\text{Current Density} = [\text{Current (A)}/\text{Electrode Area } (m^2)] \quad (13)$$

In the calculation step of linear flow rates, the calculation used to determine can be seen on Appendix Section, A.

Briefly the transformation, given in Table 3.1, is used in all flow rates, respectively:

Table 3.1. Volumetric flow rate to linear flow rate.

Volumetric Flow Rate [mL/min]	Linear Flow Rate [cm/s]
50	0.208
100	0.417
150	0.625
200	0.833

4. RESULTS

4.1. Effect of Salinity Gradient (salt ratio)

In the studies, synthetic feed salt solutions (In Figure 4.1, 1 g/L less concentrated salt solution and 30 g/L high concentrated salt solution, In Figure 4.2, 2 g/L less concentrated salt solution and 30 g/L high concentrated solution, In Figure 4.3, 1 g/L less concentrated salt solution and 45 g/L high concentrated solution) were used. As stated in previous sections, the unit of volumetric flow rate (mL/min) has been converted into a unit of linear flow rate (flow velocity) (cm/s) in order to be the basis for further studies, calculations can be checked on Appendix Section, A. During the studies, there are 5 pairs of membranes in the RED membrane stack. In order to examine the effect of the feed flow rate, the flow rates of both high concentrated salt and low concentrated salt solutions were kept equal and 4 different linear flow rates (0.208 cm/s, 0.417 cm/s, 0.625 cm/s and 0.833 cm/s) were used. Corresponding volumetric flow rates of these linear flow rate values are 50, 100, 150 and 200 mL/min respectively. Each flow rate experiment was repeated 3 times and the reliability of the data was confirmed. Electrode rinse solution flow rate is constant and is 300 mL/min in all experiments. The multiple-step chronopotentiometry graphs of the experiments can be seen on Appendix Section, B. Figure 4.1 shows the effect of feed flow rate on power density (W/m^2) for the condition that the salt ratio of less concentrated solution to high concentrated solution is 1:30. The current density is calculated by dividing the electrical current (A) taken from the system by the active membrane area (electrode area, m^2).

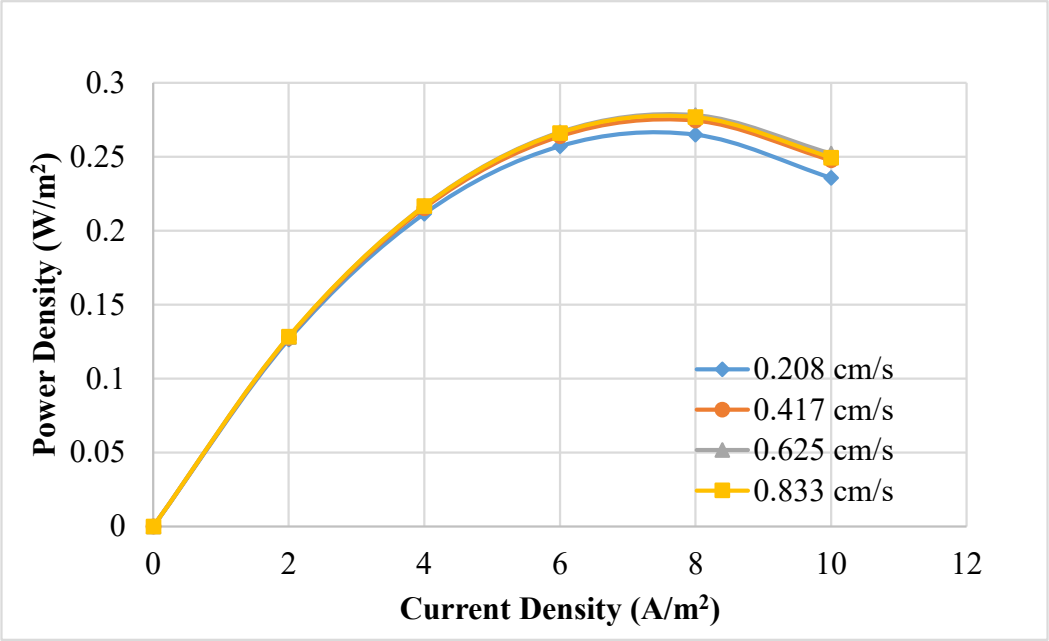

Figure 4.1. Power density values when different feed flow rates are used, 300 mL/min electrode rinse, salt ratio 1:30, 20.0 °C

Table 4.1. Maximum power density, maximum power and OCV values, salt ratio 1:30

Linear Flow Rate (cm/s)	Maximum Power Density (W/m²)	Maximum Power (W)	Open Circuit Voltage, OCV (V)
0.208 (50 mL/min)	0.265	0.026	0.740
0.417 (100 mL/min)	0.270	0.027	0.744
0.625 (150 mL/min)	0.280	0.028	0.746
0.833 (200 mL/min)	0.275	0.028	0.746

As the feed flow rate increases, the amount of ions carried through the ion exchange membranes will increase, so the generated potential difference will increase. This effect is clearly seen when the linear flow rate of the feeding solution increases from 0.208 cm/s to 0.417 cm/s, as can be seen in Table 4.1. With a linear flow rate of 0.625 cm/s, the generated power density approached 0.280 W/m^2. However, when the linear flow rate was increased further (0.833 cm/s), the residence time of the feed solutions in the membrane module was shortened, and the time for the transport of ions through the membranes was not

sufficient. This reduced the generated potential difference and hence the power density.

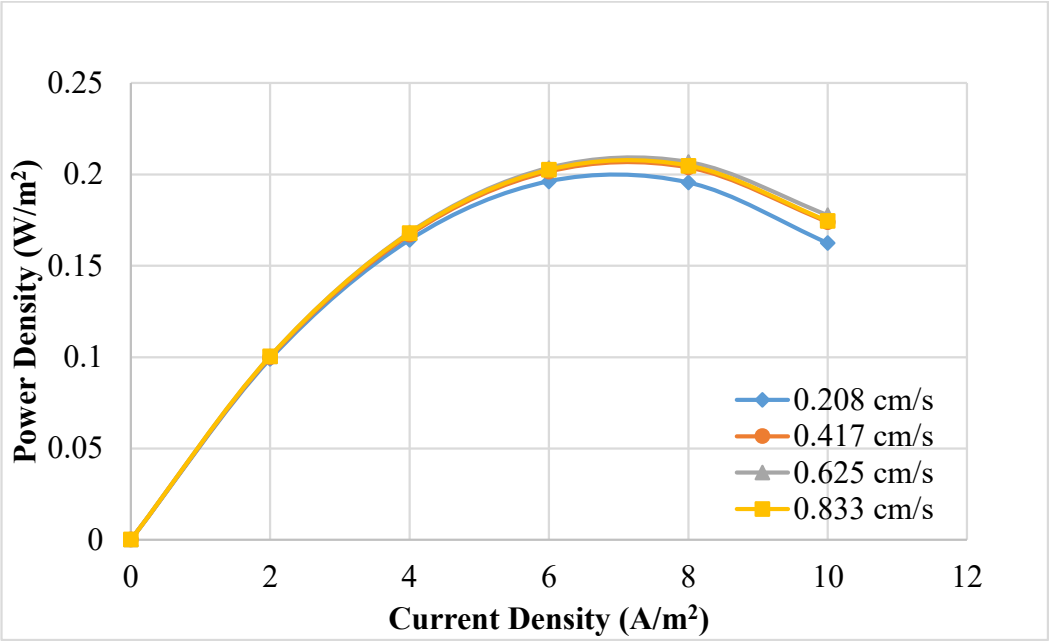

Figure 4.2. Power density values when different salt water feed flow rates are used, 300 mL/min electrode rinse, salt ratio 2:30, 20.0 °C

Table 4.2. Maximum power density, maximum power and OCV values, salt ratio 2:30

Linear Flow Rate (cm/s)	Maximum Power Density (W/m²)	Maximum Power (W)	Open Circuit Voltage, OCV (V)
0.208 (50 mL/min)	0.196	0.019	0.579
0.417 (100 mL/min)	0.204	0.020	0.582
0.625 (150 mL/min)	0.210	0.021	0.585
0.833 (200 mL/min)	0.207	0.021	0.585

Another salt ratio in which the flow rate is examined is the value of 2:30 (less concentrated salt solution:more concentrated salt solution) obtained by increasing the concentration of the less concentrated salt solution by 2 times while the concentration of the high concentrated salt solution remains the same. In this study, a lower salinity rate was applied compared to the previous study. As seen in Figure 4.2, at low salt ratio the flow rate effect decreases and the power density values converge at different flow rates. In addition, the power density has also

decreased (the effect of salt ratio is examined in the next section). As can be seen in Table 4.2, the linear flow rate is in accordance with the previous salinity rate, the optimum linear flow rate was determined as 0.625 cm/s and a power density of 0.210 W/m^2 was achieved. In addition, it is observed here that the system performance decreases at flow rates above a certain level, although the difference of maximum power density values are small.

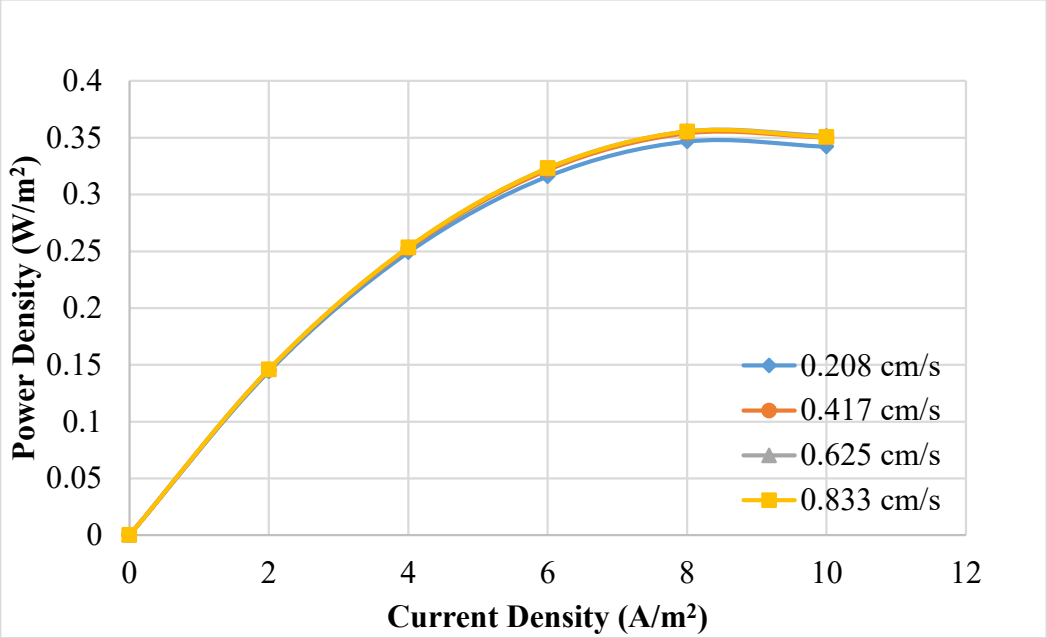

Figure 4.3. Power density values when different salt water feed flow rates are used, 300 mL/min electrode rinse, salt ratio 1:45, 20.0 °C

Table 4.3. Maximum power density, maximum power and OCV values, salt ratio 1:45.

Linear Flow Rate(cm/s)	Maximum Power Density (W/m^2)	Maximum Power (W)	Open Circuit Voltage, OCV (V)
0.208 (50 mL/min)	0.342	0.034	0.823
0.417 (100 mL/min)	0.350	0.035	0.826
0.625 (150 mL/min)	0.352	0.036	0.828
0.833 (200 mL/min)	0.350	0.036	0.828

Another salt ratio in which the flow rate is examined is the value of 1:45 (less concentrated salt solution:more concentrated salt solution) obtained by

increasing the concentration of the high salt solution and keeping the concentration of the low salt solution constant. As seen in Figure 4.3, at high salinity, the flow rate effect decreases and the power density values converge again at different flow rates. Power density values have also increased with respect to 1:30 and 2:30 salt ratios. As can be seen in Table 4.3, the optimum linear flow rate was determined as 0.625 cm/s and a power density of 0.352 W/m^2 was achieved, with the flow rates in accordance with the previous salt ratio. This shows that the salt ratio has a more dominant effect than the change in the flow rate, verified also in this salinity study. In addition, it has been observed here that the system performance decreases at flow rates above a certain level (greater than 0.625 cm/s), although the difference is small.

According to Nernst equation (Equation 5), the theoretical potential difference that can be produced on both sides of the membrane depends on and is directly proportional to the salinity gradient (difference). In Figure 4.4, three different salt ratios (1:30, 2:30, 1:45) are examined. In this study, the concentration of the more saline solution was changed to 30 g/L and 45 g/L, and the concentration of the less saline solution to 1 g/L and 2 g/L. Each study was repeated 3 times to be evaluated for consistency and accuracy. Data are plotted according to average results.

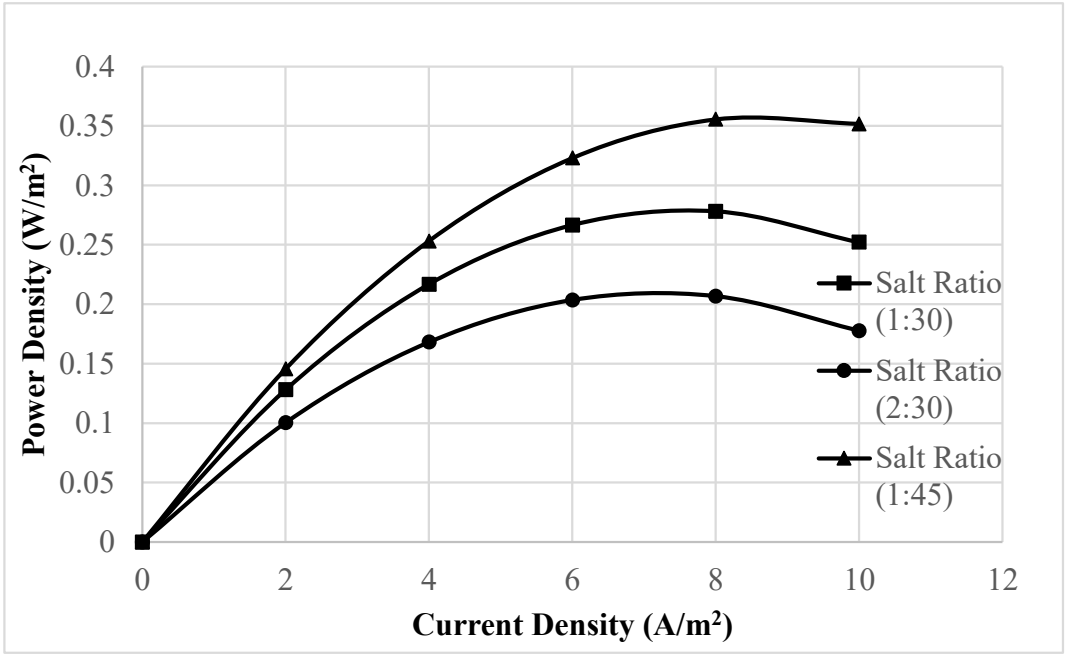

Figure 4.4. The comparison of optimum power density values for different salt ratio studies at determined optimum linear flow rate value, 0.625 cm/s.

Table 4.4. Maximum power density, maximum power and OCV values at optimum linear flow rate, comparison of salt ratio

Salt Ratio (g/L : g/L) 0.625 cm/s	Maximum Power Density (W/m^2)	Maximum Power (W)	Open Circuit Voltage, OCV (V)
1:30	0.280	0.028	0.746
2:30	0.210	0.021	0.585
1:45	0.352	0.036	0.828

As expected Figure 4.4 shows that as the salinity increases the potential difference produced increases and therefore the power density increases. The highest power density values achieved in these data are given in Table 4.4 together with the optimum flow rates.

In Figure 4.5, the average open circuit voltage (OCV) values for different salt ratio conditions at optimum linear flow rate can be seen.

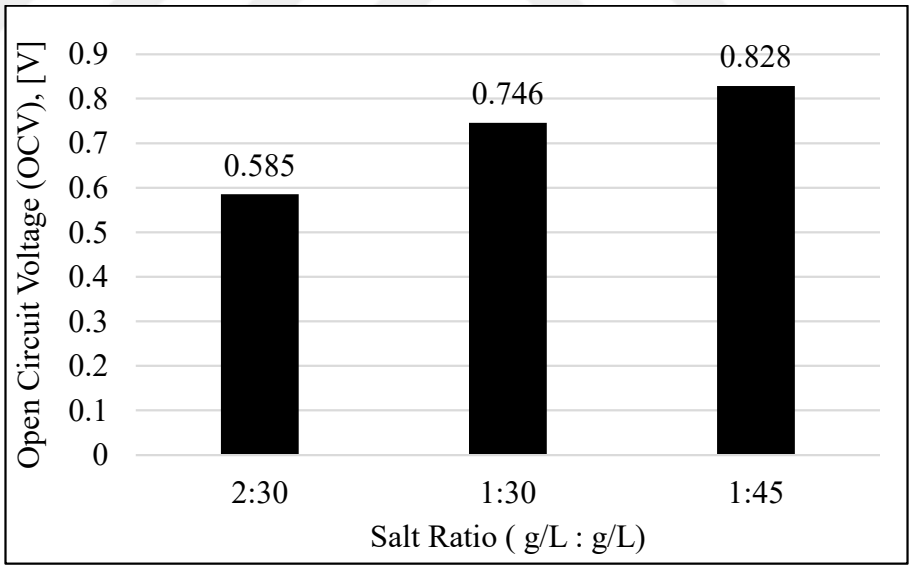

Figure 4.5. The average open circuit voltage (OCV) values of the RED membrane stack for different salt ratio values at optimum linear flow rate, 0.625 cm/s, electrode rinse water flow rate: 300 mL/min (Temperature: 20°C)

4.2. Effect of Flow Rate

During the studies, there are 3, 5, 7 and 10 pairs of membranes in the RED membrane stack. In order to examine the effect of feed flow rate, the flow rates of both more concentrated and less concentrated saline solutions were kept equal and 4 different linear flow rates (0.208 cm/s, 0.417 cm/s, 0.625 cm/s and 0.833 cm/s) were used. The volumetric flow rate equivalents of these linear flow rate values are 30, 60, 90, 120 mL/min for 3 pairs of membranes, respectively. The volumetric flow rate equivalents of these linear flow rate values are 50, 100, 150, 200 mL/min for 5 pairs of membranes, respectively. The volumetric flow rate equivalents of the specified linear flow rate values are 70, 140, 210, 280 mL/min for 7 pairs of membranes, respectively. Volumetric flow rate equivalents for 10 pairs of membranes used in RED membrane stack are 100, 200, 300, 400 mL/min. Each flow rate experiment was repeated for 3 times and the reliability of the data was confirmed. Electrode rinse solution flow rate is constant and 300 mL/min in all experiments. The multiple-step chronopotentiometry graphs of the experiments can be seen on Appendix Section, C.

The effect of feed flow rate on power density (W/m^2) is shown on the figures. The current density is calculated by dividing the electrical current (A) taken from the system by the active membrane area (electrode area) (m^2).

In Figure 4.6, when 3 pairs of membranes are used in the RED membrane stack, the power density versus current density graph for 1:30 (g/L:g/L) salt ratio is given.

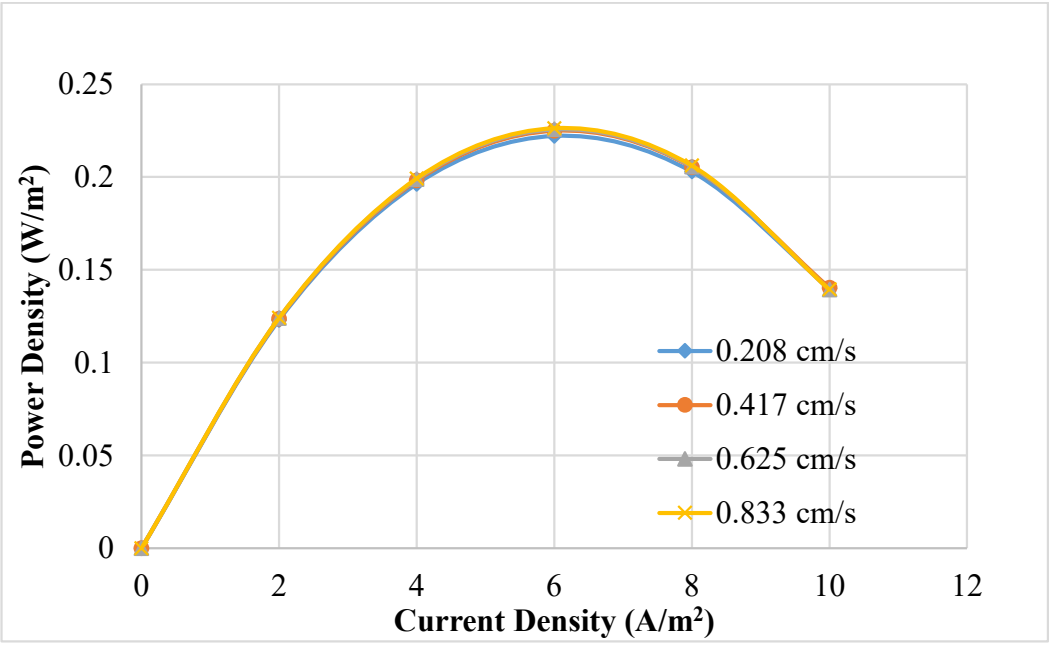

Figure 4.6. Comparison of power density values for RED stack with 3 pairs of membranes, different linear flow rate values, electrode rinse solution flow rate: 300 mL/min, salt ratio: 1:30 (Temperature: 20 °C)

When 3 pairs of membranes are used, maximum power densities achieved in studies performed at different speeds with salt ratio of 1:30 are given in Table 4.5.

Table 4.5. Maximum power density values obtained from different flow rates for 3 pairs of membranes, salt ratio: 1:30

Linear Flow Rate (cm/s)	**Maximum Power Density (W/m^2)**
0.208 (30 mL/min)	0.222
0.417 (60 mL/min)	0.224
0.625 (90 mL/min)	0.225
0.833 (120 mL/min)	0.226

When using 3 pairs of membranes at every 4 flow rates, the highest power density result was determined as 0.226 W/m^2 with a flow rate of 0.833 cm/s according to the maximum power densities achieved (Figure 4.6).

In Figure 4.7, when 5 pairs of membranes are used in the RED membrane stack, the power density versus the current density graph for the salt ratio of 1:30 (g/L:g/L) is given.

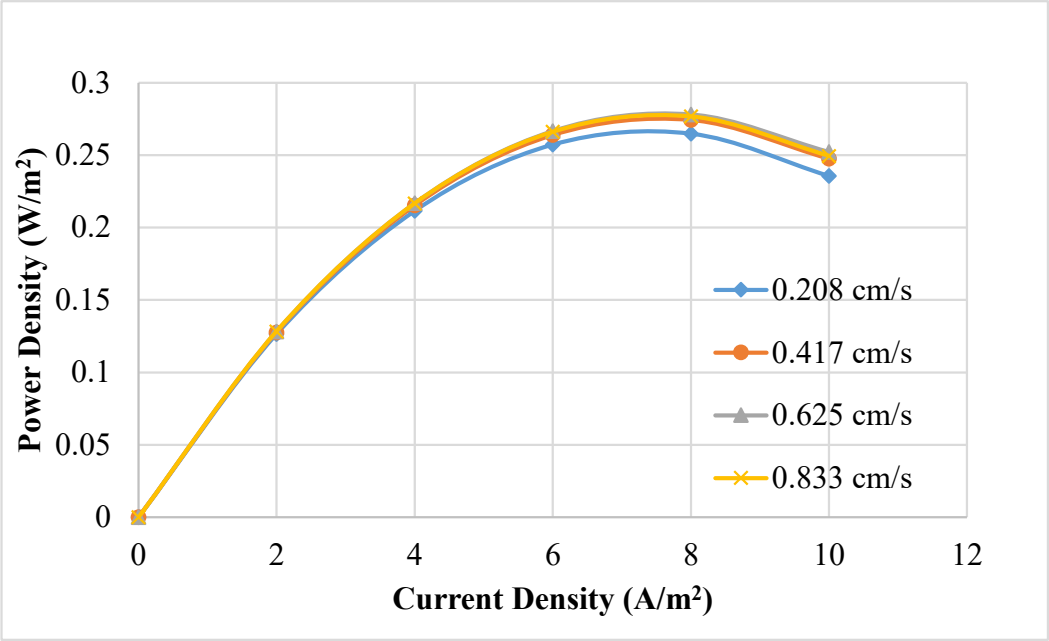

Figure 4.7. Comparison of power density values for RED stack with 5 pairs of membranes, different linear flow rate values, electrode rinse solution flow rate: 300 mL/min, salt ratio: 1:30 (Temperature: 20 °C)

When 5 pairs of membranes are used, the maximum power densities achieved in studies performed at different speeds using salt ratio of 1:30 are given in Table 4.6.

Table 4.6. Maximum power density values obtained from different flow rates for 5 pairs of membranes, salt ratio: 1:30

Linear Flow Rate (cm/s)	Maximum Power Density (W/m²)
0.208 (50 mL/min)	0.265
0.417 (100 mL/min)	0.270
0.625 (150 mL/min)	0.280
0.833 (200 mL/min)	0.275

When using 5 pairs of membranes at every 4 flow rates, the best result was determined as 0.278 W/m^2 with a flow rate of 0.625 cm/s according to the maximum power densities achieved (Figure 4.7).

In Figure 4.8, when 7 pairs of membranes are used in the RED membrane stack, the power density vs current density graph is given for the salinity ratio of 1:30 (g/L:g/L).

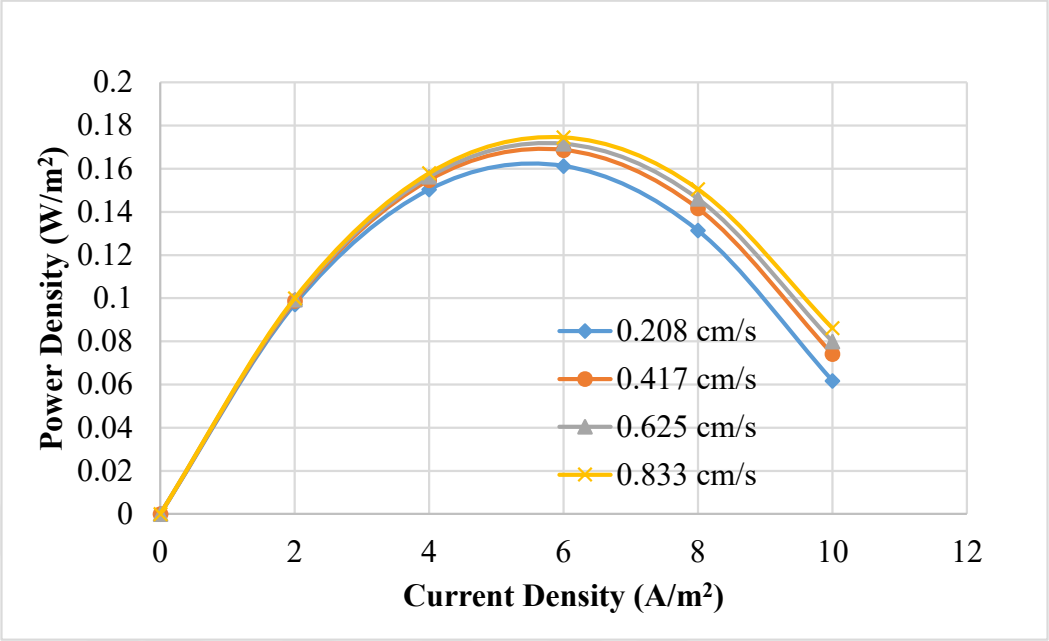

Figure 4.8. Comparison of power density values for RED stack with 7 pairs of membranes, different linear flow rate values, electrode rinse solution flow rate: 300 mL/min, salt ratio: 1:30 (Temperature: 20°C)

When 7 pairs of membranes are used, the maximum power densities achieved in studies performed at different speeds using salt ratio of 1:30 are given in Table 4.7.

Table 4.7. Maximum power density values obtained from different flow rates for 7 pairs of membranes, salt ratio: 1:30

Linear Flow Rate (cm/s)	Maximum Power Density (W/m^2)
0.208 (70 mL/min)	0.161
0.417 (140 mL/min)	0.169
0.625 (210 mL/min)	0.172
0.833 (280 mL/min)	0.175

When using 7 pairs of membranes at every 4 flow rates, the best result was determined as 0.175 W/m^2 with a flow rate of 0.833 cm/s according to the maximum power densities achieved (Figure 4.8).

In Figure 4.9, when 10 pairs of membranes are used in the RED membrane stack, the power density versus current density graph obtained for 1:30 (g/L:g/L) salinity ratio is given.

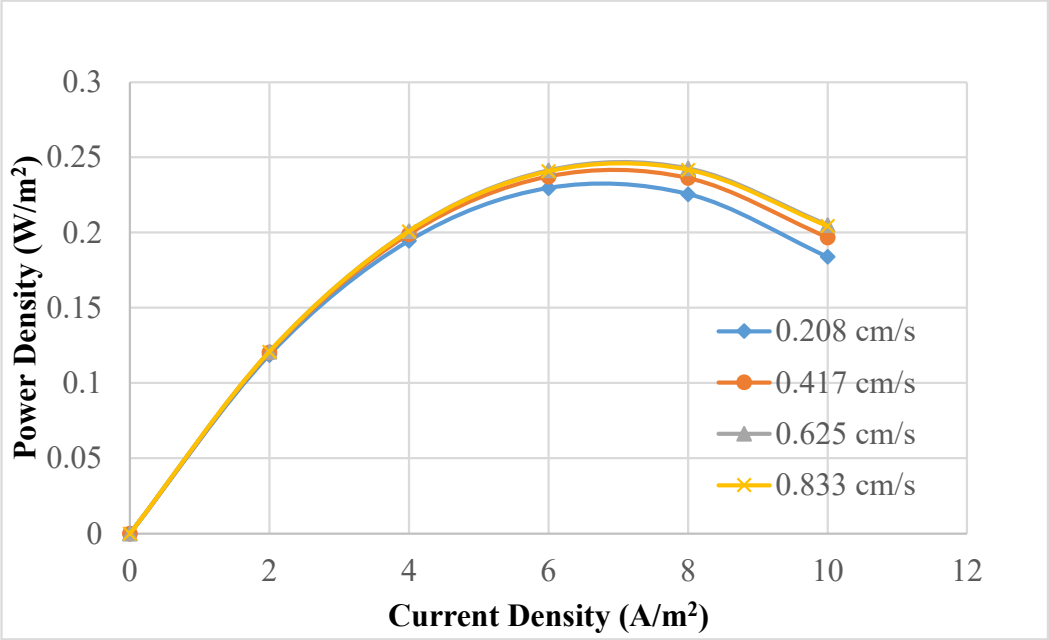

Figure 4.9. Comparison of power density values for RED stack with 10 pairs of membranes, different linear flow rate values, electrode rinse solution flow rate: 300 mL/min, salt ratio: 1:30 (Temperature: 20°C)

When 10 pairs of membranes are used, the maximum power densities achieved in studies performed at different speeds using salt ratio of 1:30 are given in Table 4.8.

Table 4.8. Maximum power density values obtained from different flow rates for 10 pairs of membranes, salt ratio: 1:30

Linear Flow Rate (cm/s)	**Maximum Power Density (W/m^2)**
0.208 (100 mL/min)	0.230
0.417 (200 mL/min)	0.237
0.625 (300 mL/min)	0.243
0.833 (400 mL/min)	0.242

When using 10 pairs of membranes at every 4 flow rates, comparing all the maximum power densities, the best result was determined as 0.243 W/m^2 with a flow rate of 0.625 cm/s according to the maximum power densities obtained (Figure 4.9).

In addition, the graphs of power vs. current were also drawn, and the power values generated in each number of membrane pairs were examined. Figure 4.10 shows the power versus current obtained for a (g/L:g/L) salt ratio of 1:30 when 3 pairs of membranes are used in the RED membrane stack.

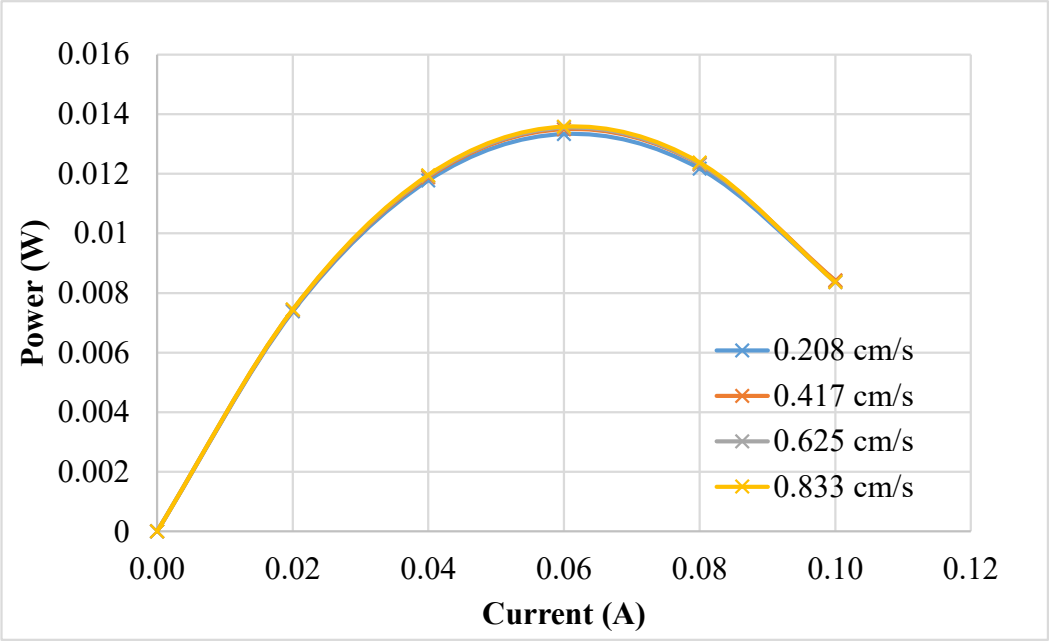

Figure 4.10. Comparison of power values for RED stack with 3 pairs of membranes, different linear flow rate values, electrode rinse solution flow rate: 300 mL/min, salt ratio: 1:30 (Temperature: 20 °C)

When 3 pairs of membranes are used, the maximum power values achieved in studies performed at different speeds using-salt ratio of 1:30 are given in Table 4.9.

Table 4.9. Maximum power values obtained from different flow rates for 3 pairs of membranes

Linear Flow Rate (cm/s)	Maximum Power (W)
0.208 (30 mL/min)	0.01332
0.417 (60 mL/min)	0.01349
0.625 (90 mL/min)	0.01354
0.833 (120 mL/min)	0.01358

When using 3 pairs of membranes at each flow rate of 4 flows, according to the maximum power values achieved (Figure 4.10), the highest power was determined as 0.01358 W with a flow rate of 0.833 cm/s.

In Figure 4.11, when 5 pairs of membranes are used in the RED membrane stack, the plot of power vs current obtained for a salt ratio of 1:30 (g/L:g/L) is given.

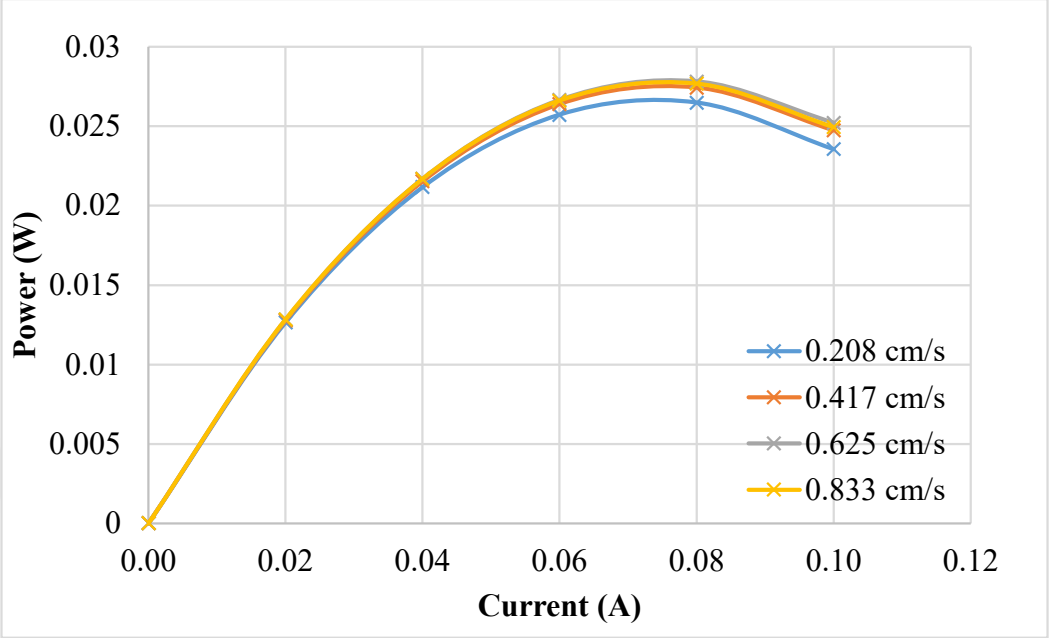

Figure 4.11. Comparison of power values for RED stack with 5 pairs of membranes, different linear flow rate values, electrode rinse solution flow rate: 300 mL/min, salt ratio: 1:30 (Temperature: 20°C)

When 5 pairs of membranes are used, the maximum power values achieved in studies performed at different speeds using 1:30 salt ratio are given in Table 4.10.

Table 4.10. Maximum power values obtained from different flow rates for 5 pairs of membranes

Linear Flow Rate (cm/s)	Maximum Power (W)
0.208 (50 mL/min)	0.02648
0.417 (100 mL/min)	0.02743
0.625 (150 mL/min)	0.02781
0.833 (200 mL/min)	0.02768

When using 5 pairs of membranes at every 4 flow rates, the best result of power was determined as 0.02781 W with a flow rate of 0.625 cm/s according to the maximum power values achieved (Figure 4.11). Figure 4.12 shows the power versus current obtained for a salt ratio of 1:30 (g/L:g/L) when 7 pairs of membranes are used in the RED membrane stack.

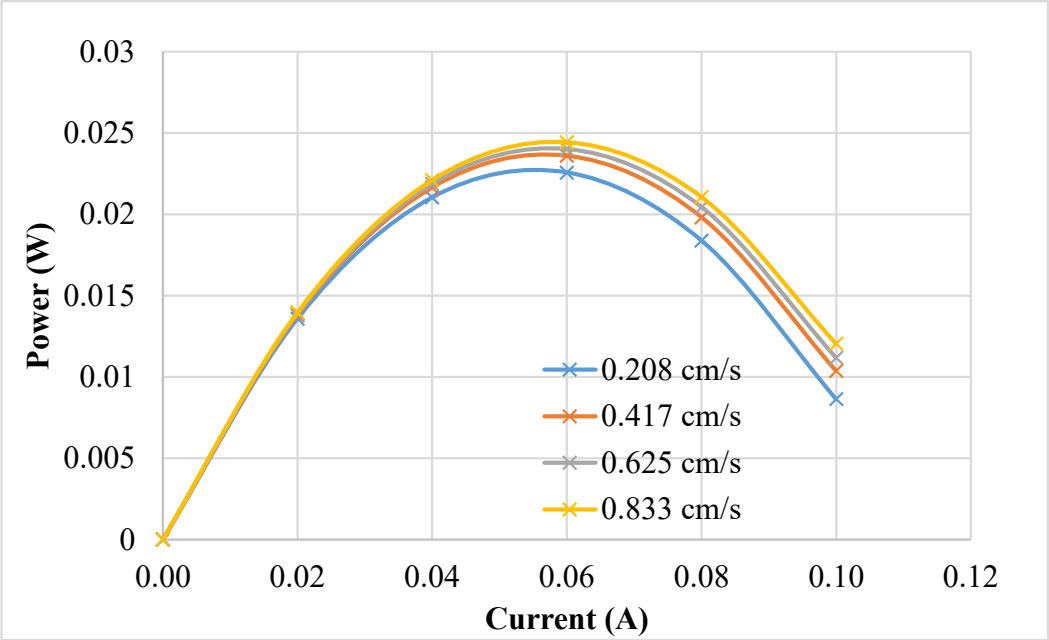

Figure 4.12. Comparison of power values for RED stack with 7 pairs of membranes, different linear flow rate values, electrode rinse water flow rate: 300 mL/min, salt ratio: 1:30 (Temperature: 20°C)

When 7 pairs of membranes are used, the maximum power values achieved in studies performed at different speeds using a salt ratio of 1:30 are given in Table 4.11.

Table 4.11. Maximum power values obtained from different flow rates for 7 pairs of membranes

Linear Flow Rate (cm/s)	Maximum Power (W)
0.208 (70 mL/min)	0.02257
0.417 (140 mL/min)	0.02361
0.625 (210 mL/min)	0.02402
0.833 (280 mL/min)	0.02443

When using 7 pairs of membranes at every 4 flow rates, the best result according to the maximum power value obtained (Figure 4.12) was determined as 0.02443 W with a flow rate of 0.833 cm/s.

Figure 4.13 shows the power versus current obtained for a salt ratio of 1:30 (g/L:g/L) when 10 pairs of membranes are used in the RED membrane stack.

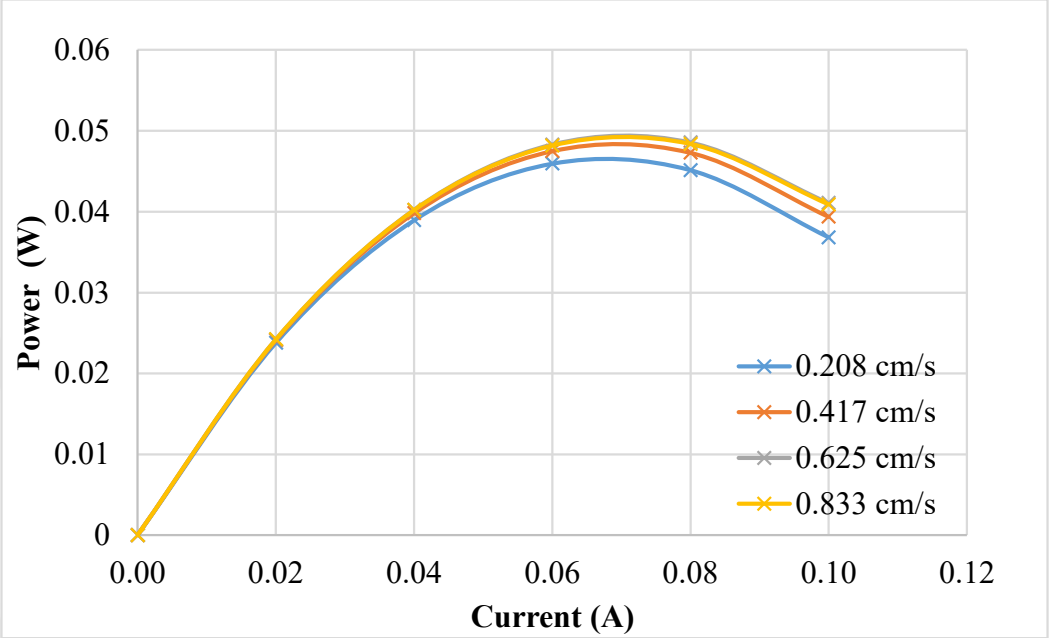

Figure 4.13. Comparison of power values for RED stack with 10 pairs of membranes, different linear flow rate values, electrode rinse solution flow rate: 300 mL/min, salt ratio: 1:30 (Temperature: 20 °C)

Maximum power values achieved in studies performed at different speeds using a salt ratio of 1:30 when 10 pairs of membranes are used are given in Table 4.12.

Table 4.12. Maximum power values obtained from different flow rates for 10 pairs of membranes

Linear Flow Rate (cm/s)	Maximum Power (W)
0.208 (100 mL/min)	0.04593
0.417 (200 mL/min)	0.04727
0.625 (300 mL/min)	0.04854
0.833 (400 mL/min)	0.04836

When using 10 pairs of membranes at every 4 flow rates, the best result was determined as 0.04854 W with a flow rate of 0.625 cm/s according to the maximum power values obtained (Figure 4.13).

Furthermore, the data for open circuit voltage (OCV) were obtained for every study and given in Table 4.13.

Table 4.13. Open circuit voltage (OCV) values for given parameters.

Linear Flow Rate (cm/s)	**Open Circuit Voltage, OCV (V)**			
	3 pairs	**5 pairs**	**7 pairs**	**10 pairs**
0.208	0.444	0.740	0.834	1.399
0.417	0.445	0.744	0.839	1.411
0.625	0.446	0.746	0.840	1.414
0.833	0.446	0.746	0.840	1.414

Detailed graph regarding the effect of the number of membrane pairs to OCV values are given in next section.

4.3. Effect of Number of Membrane Pairs

In this section, the data obtained in previous section has been used. The graphs of voltage vs. current are drawn according to the optimum linear flow rate, which was determined as 0.625 cm/s, can be seen in Figure 4.14.

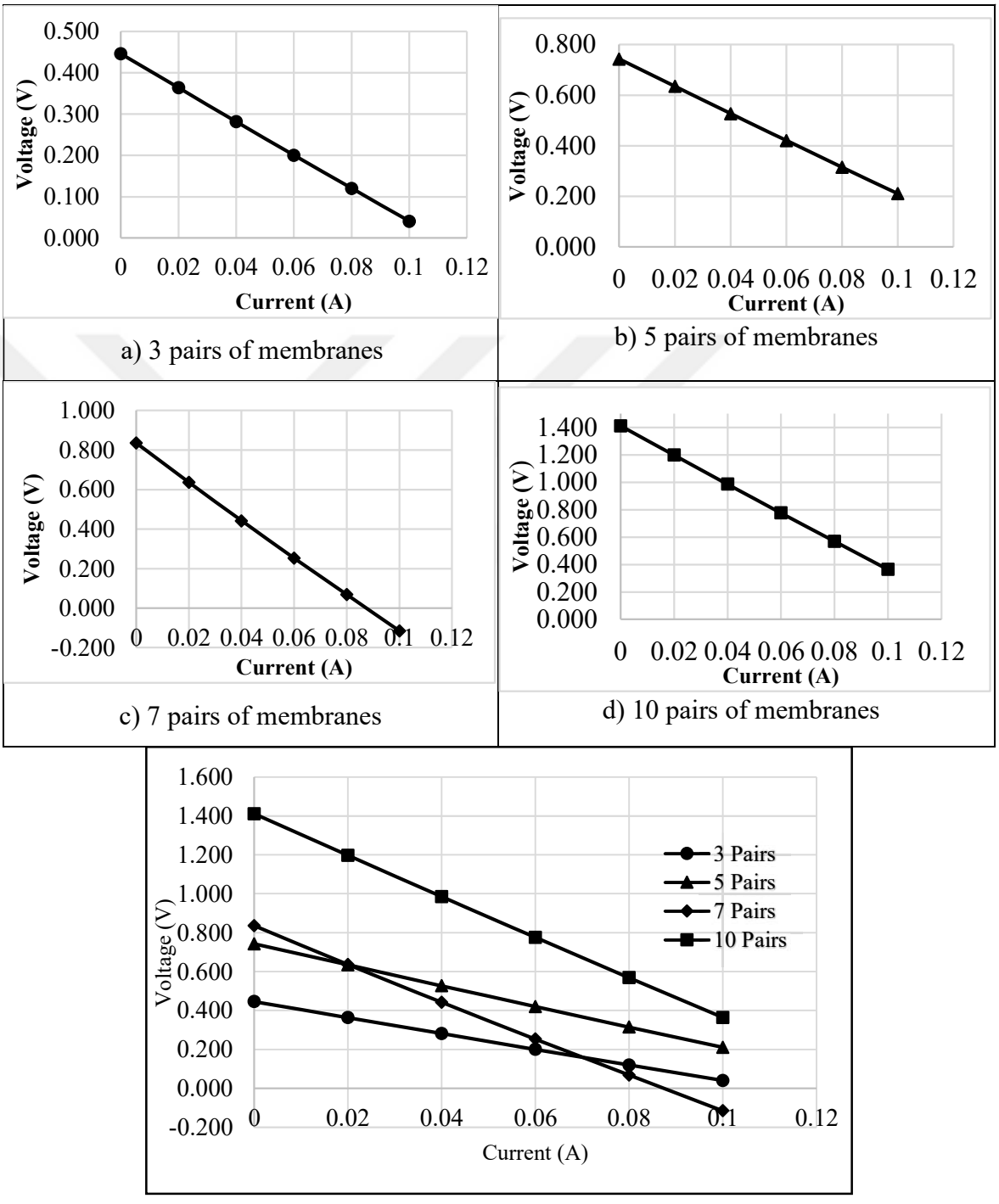

Figure 4.14. Voltage versus current graphs of RED membrane stack having a) 3 pairs of membranes, b) 5 pairs of membranes, c) 7 pairs of membranes, d) 10 pairs of membranes are used, all graphs are combined at bottom, at optimum linear flow rate, which was determined as 0.625 cm/s, electrode rinse solution flow rate: 300 mL/min, salt ratio: 1:30 (Temperature: 20 °C)

Figure 4.15 shows the effect of number of membrane pairs on open circuit voltage (OCV) values at optimum flow rate:

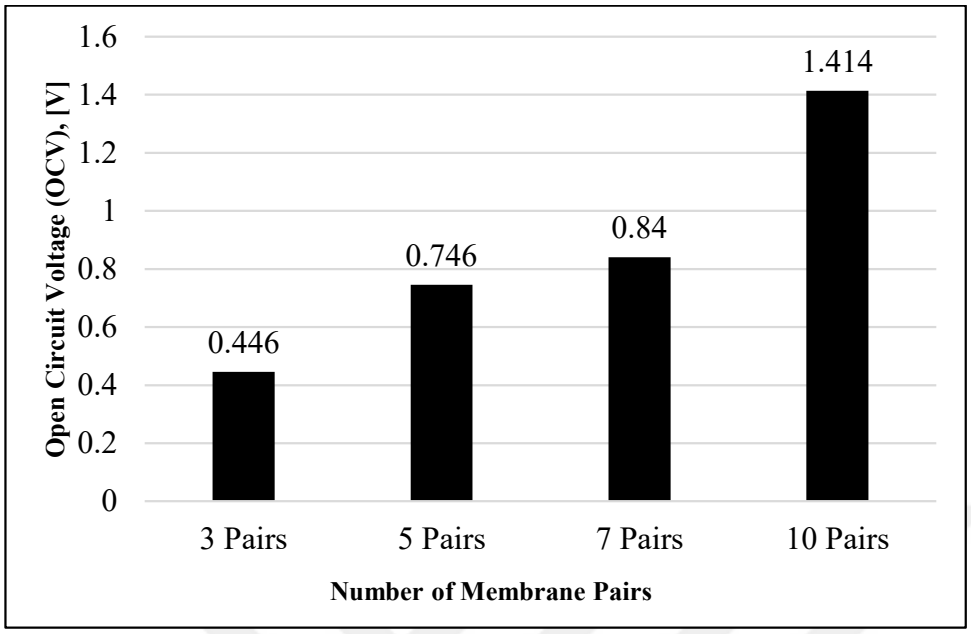

Figure 4.15. The average open circuit voltage (OCV) values of the RED membrane stack at optimum flow rate, electrode rinse solution flow rate: 300 mL/min, salt ratio: 1:30 (Temperature: 20 °C)

When it is desired to examine the change of power density values with different numbers of membrane pairs at given same flow rates, can be seen in Figure 4.16.

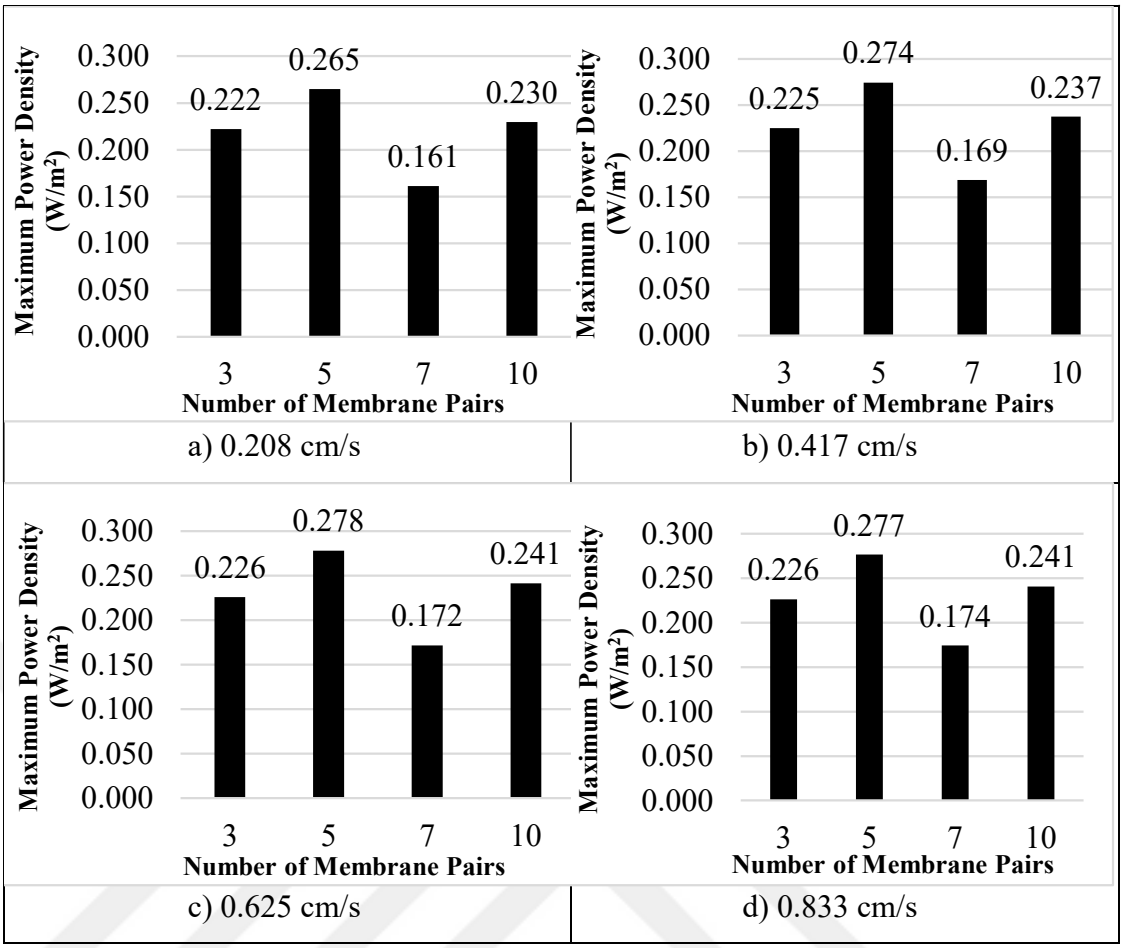

Figure 4.16. The maximum power density values of RED membrane stack having different numbers of membrane pairs at same linear flow rates, a) 0.208 cm/s, b) 0.417 cm/s, c) 0.625 cm/s, d) 0.833 cm/s, electrode rinse solution flow rate: 300 mL/min, salt ratio: 1:30 (Temperature: 20 °C)

According to Figure 4.16, effect of membrane pair number on maximum power densities can not be clearly seen. The differences can be seen more clearly in Figure 4.17, where the maximum power values produced are examined.

When it is desired to examine the change of generated maximum power values with different numbers of membrane pairs at given same flow rates, can be seen in Figure 4.17:

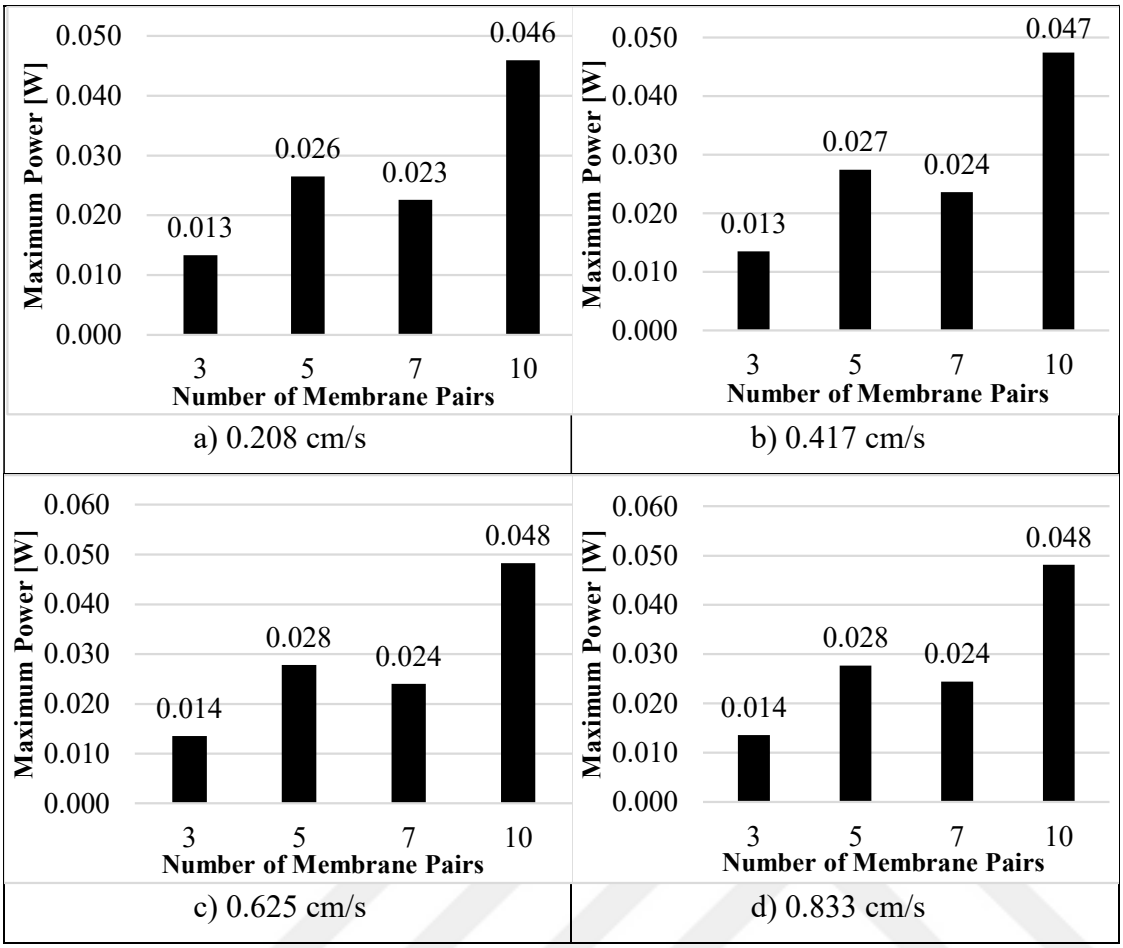

Figure 4.17. The maximum power values of RED membrane stack having different numbers of pairs at same linear flow rates, a) 0.208 cm/s, b) 0.417 cm/s, c) 0.625 cm/s, d) 0.833 cm/s, electrode rinse solution flow rate: 300 mL/min, salt ratio: 1:30 (Temperature: 20 °C)

5. DISCUSSION

When different salt ratios were examined at optimum feed flow rate, electrical power densities of 0.280, 0.210 and 0.352 W/m^2 were obtained using salt ratios of 1:30, 2:30 and 1:45, respectively. It has been observed that when the salinity gradient is increased, the generated power density increases. When the salinity gradient was increased from 2:30 to 1:30, an increase of 33% was obtained in the power density. When the salinity gradient was increased from 1:30 to 1:45, an increase of 26% was obtained in the generated power density. When the salinity gradient was increased from 2:30 to 1:45, an increase of 68% was obtained in the power density produced.

Another important point to be stated here is that the salt concentration in the low saline solution should not fall below a certain value. Otherwise, feeding very dilute solutions to the system will increase the electrical resistance of the membrane stack in RED system and this will decrease the electrical potential value.

While discussing the resistance concept, the decrease of power density after reaching peak point which can be seen on power density versus current density graphs complies with the decreasing concept in voltage versus current graphs. Increasing the current delivered from system causing the voltage drop because of simultaneous increase in the internal resistance of cell.

Comparing the flow rate effect results, ex. 10 pairs of membranes in stack, as the maximum power and power density values, at a flow rate of 0.625 cm/s, a maximum power generation of 0.049 W and a power density of 0.243 W/m^2 were obtained, and due to lower values obtained at 0.833 cm/s of flow rate, a maximum power generation of 0.048 W and a power density of 0.242 W/m^2, the optimum linear flow rate values revealed in the previous study were also confirmed, complying with the other studied numbers of membrane pairs.

When the number of membrane pairs is increased from 7 to 10, the maximum power value has increased by 100%. The reason why the increase in the number of membranes cannot be seen clearly on the power density graphs is that the generated power is divided by the membrane area.

The increase in the feed flow rate increased the maximum generated power values, but it showed that the high flow rate did not increase the maximum power

values generated after a certain point on the system performance, and obtained nearly the same or lesser power values, ex. the difference between linear flow rate values of 0.625 cm/s and 0.833 cm/s. Comparing the salinity and flow rate parameters show that the salinity has more dominant effect on system.

When open circuit voltage (OCV) values are examined, as the number of membrane pairs is increased, the open circuit voltage (OCV) also increases, revealing the highest voltage values obtained at zero current value. Highest OCV value obtained was 1.414 V for 10 pairs of membranes. The open circuit voltage (OCV) can be explained by the Nernst equation, and it is directly proportional to the number of membranes in the equation. Therefore, it can be accepted that the increase in the number of membranes has a direct effect on the OCV value. It was concluded that in parallel with the increase in the number of membrane pairs, there was an increase in their potential values.

Considering the OCV values, increasing the number of membrane pairs used in the membrane stack from 7 pairs to 10 pairs shows an increase of 68.33% in the OCV value reached.

The effects of the number of membrane pairs on the maximum power values can be clearly seen, and it is noteworthy that if the number of membrane pairs is increased, the maximum power that can be produced increases. This situation does not make a clear difference when the number of membrane pairs is increased from 5 to 7, but it reveals a similar situation when 3 to 7 or 7 to 10 membrane pairs are examined.

As the feed flow rate increases, the amount of ions carried through the ion exchange membranes will increase, so the generated potential difference will also increase. This effect is clearly seen when the linear flow rate of the feed solution increases from 0.208 cm/s to 0.417 cm/s, or when it increases to 0.625 cm/s. With a linear flow rate of 0.625 cm/s, the maximum power generated, in 10 pairs of membranes, reached 0.049 W and the maximum power density reached 0.243 W/m^2. However, when the linear flow rate was increased further (0.833 cm/s), the residence time of the feed solutions in the membrane module was shortened, and the time for the transport of ions through the membranes was not sufficient. This reduced the generated potential difference and hence the maximum generated power value.

6. CONCLUSIONS and RECOMMENDATIONS

In order to observe the parameters in the RED system, firstly the system is designed and set-up as a lab scale system. High concentrated and less concentrated salt solutions were prepared using NaCl and the effects of feed flow rates, salt ratio, and the number of membrane pairs were examined as the most basic parameters in the experimental studies. Increasing the feed flow rate increased the power density generated, but it was found that the high flow rate negatively affected the system performance (with the decrease in power density). As a result of the studies, the optimum feed flow rate was determined as 150 mL/min and the linear flow rate was 0.625 cm/s in the designed process. When the results are evaluated, it is found out that generation of salinity gradient energy via reverse electrodialysis (RED) process is operating successfully.

Considering the experiments, with the increase of the number of membrane pairs the effect of flow rate can be seen better. The effect of flow rate is not so clear considering the 3 pairs of membranes in cell, but if 7 pairs of membranes or 10 pairs of membranes are stacked and examined, the effect is clearer.

Using thinner spacers (for example, <200 micrometers) instead of 400 micrometers thickness, the effect of flow rate can be examined more prominently. The main reason for this phenomenon is the effect of spacer on the electrical resistance of membrane stack. The thinner the spacer is, the lesser electrical resistance presence in the membrane stack. Observation of different parameters is easier when the resistance of stack is lower.

In addition, explaining some parameters that may affect the system is important. The calibration process should be done when there is any physical intervention on the measuring device (when the system is moved, the power line and ground line changes) or if the device gives any message about the calibration of the program. It is important to calibrate the instrument, otherwise the results would be different than expected. Experimental studies were carried out in an air-conditioned environment (20 °C), thus conducting the experiments in a different temperature level may affect the results.

In future research, different membranes and different spacer configurations can be investigated. Pilot tests of the designed process can be examined. Different number of membranes in stack, different flow rates for both saline flows and

electrode rinse flows, and multi-stage performance can be examined. Production of different RED membranes is another topic that can be focused on, which later can be used on the trials of these membranes in RED stack. Experimental design parameters can be examined via different computational programs. Fouling of membranes in the system is another topic which can be investigated. The system can be fed with non artificial feed solutions. Instead of measuring flow rates manually, digital flowmeters can be integrated into process flow diagram.

REFERENCES

Alvarez-Silva, O.A., Osorio, A.F., Winter, C. (2016). Practical global salinity gradient energy potential. Renew. Sustain. Energy Rev., vol. 60, p. 1387-1395.

Bharadwaj, D., Fyles, T. M., & Struchtrup, H. (2016). Multistage Pressure-Retarded Osmosis. Journal of Non-Equilibrium Thermodynamics, vol. 41, p. 4.

Cipollina, A., Micale, G. (2016). Sustainable Energy from Salinity Gradients, Elsevier.

Długołęcki P., Gambier A., Nijmeijer K., Wessling M. (2009). Practical potential of reverse electrodialysis as process for sustainable energy generation. Environmental Science & Technology, vol. 43, p. 6888-6894.

Długołecki, P., Nijmeijer, K., Metz, S., Wessling, M. (2008). Current status of ion exchange membranes for power generation from salinity gradients, Journal of Membrane Science, vol. 319, p. 214-222.

Fouad Saad. (2016). The Shock of Energy Transition, Partridge Publishing.

Gamry Reference 3000 Potentiostat/Galvanostat/ZRA n.d. https://www.gamry.com/potentiostats/reference-3000/ (accessed March 8, 2019).

Gilstrap, M.C. (2013). Renewable Electricity Generation From Salinity Gradients Using Reverse Electrodialysis, MSc. Thesis, Georgia Institute of Technology.

Guler, E. (2014). Anion exchange membrane design for reverse electrodialysis. PhD. Thesis. Universiteit Twente.

Hong, J.G., Gao, H., Gan, L., Tong, X., Xiao, C., Liu, S., Zhang, B., Chen, Y. (2019). Chapter 13: Nanocomposite and nanostructured ion exchange membrane in salinity gradient power generation using reverse electrodialysis. In Advanced Nanomaterials for Membrane Synthesis and Its Applications; Elsevier B.V.: Amsterdam, The Netherlands, p. 295-316.

Jagur-Grodzinskr J., Kramer R. (1986). Novel Process for Direct Conversion of Free Energy of Mixing into Electric Power. Ind. Eng. Chem. Process Des. Dev.

Jones, A., Finley W. (2003). Recent development in salinity gradient power. OCEANS. Proc., vol. 4, IEEE; 200: p. 2284–7.

Kuleszo, J., Kroeze, C., Post, J., & Fekete, B. M. (2010). The potential of blue energy for reducing emissions of CO2 and non-CO2 greenhouse gases. Journal of Integrative Environmental Sciences, 7(sup1), 89-96.

Lacey R.E. (1980). Energy by reverse electrodialysis. Ocean Eng.

Mei, Y., Tang, C.Y. (2018). Recent developments and future perspectives of reverse electrodialysis technology: A review, Desalination 425, 156-174.

Micale, G., Cipollina, A., Tamburini, A. (2016). Chapter 1: Salinity gradient energy. In Sustainable Energy from Salinity Gradients, Elsevier, B.V., Amsterdam, The Netherlands, p. 1-18.

Ohshima H., Ohki S. (1985). Donnan potential and surface potential of a charged membrane. Biophys J.

Ortiz-Imedio, R., Gomez-Coma, L., Fallanza, M., Ortiz, A., Ibañez, R., Ortiz I. (2019). Comparative performance of Salinity Gradient Power-Reverse Electrodialysis under different operating conditions, Desalination, vol. 457, p. 8-21.

Pattle, R.E. (1954). Production of Electric Power by mixing Fresh and Salt Water in the Hydroelectric Pile. Nature, vol. 174, p. 660.

Pawlowski, S. (2015). Experimental and modeling studies on reverse electrodialysis for sustainable power generation (Doctoral Dissertation, Universidade NOVA de Lisboa, Lisbon, Portugal).

Post J.W., Hamelers H.V.M., Buisman C.J.N. (2008). Energy recovery from controlled mixing salt and fresh water with a reverse electrodialysis system. Environ. Sci. Technol., vol. 42, p. 5785-5790.

Rijnaarts T. (2018). The role of membranes in the use of natural salinity gradients for reverse electrodialysis. PhD Thesis. University of Twente.

Rijnaarts, T., Moreno, J., Saakes, M., de Vos, W.M., Nijmeijer, K. (2019). Role of anion exchange membrane fouling in reverse electrodialysis using natural feed waters, Colloids and Surfaces A: Physicochemical and Engineering Aspects, vol. 560, p. 198-204.

Schaetzle, O., Buisman, C. J. N. (2015). Salinity Gradient Energy: Current State and New Trends. Engineering, vol. 1(2), p. 164-166.

Simões, C., Pintossi, D., Saakes, M., Brilman, W. (2021). Optimizing multistage reverse electrodialysis for enhanced energy recovery from river water and seawater: Experimental and modeling investigation, Advances in Applied Energy, vol. 2, 100023.

Skråmestø, Ø.S.Ø., Skilhagen, S.S.E., Nielsen, W.K.W. (2009). Power Production Based on Osmotic Pressure. Waterpower XVI, p. 1-9.

Tufa, R.A., Pawlowski, S., Veerman, J., Bouzek, K., Fontananova, E., di Profio, G., Velizarov, S., Crespo, J.G., Nijmeijer, K., Curcio, E. (2018). Progress and prospects in reverse electrodialysis for salinity gradient energy conversion and storage, Applied Energy, vol. 225, p. 290-331.

Veerman, J., Saakes, M., Metz, S.J., Harmsen, G.J. (2010). Reverse electrodialysis: Evaluation of suitable electrode systems, Journal of Applied Electrochemistry, vol. 40, p. 1461-1474.

Veerman, J., Post, J.W., Saakes, M., Metz, S.J., Harmsen, G.J. (2008). Reducing power losses caused by ionic shortcut currents in reverse electrodialysis stacks by a validated model, Journal of Membrane Science, vol. 310, p. 418-430.

Vermaas, D.A., Veerman, J., Saakes, M., Nijmeijer, K. (2014). Influence of multivalent ions on renewable energy generation in reverse electrodialysis. Energy Environ. Sci., vol. 7(4), p. 1434-1445.

Weinstein, J.N., Leitz, F.B.J.W. (1976). Electric power from differences in salinity: the dialytic battery, Science, vol. 191, p. 557-559.

ACKNOWLEDGEMENTS

This study has been financially supported by bilateral collaboration of the Scientific and Technological Research Council of Turkey and Poland (TÜBİTAK-NCBR-2549, Project No: TÜBİTAK-MAG-117M023). I am grateful to TÜBİTAK for support and scholarship during the thesis study.

I would like to thank my supervisors Prof. Dr. Nalan KABAY and Dr. Enver GÜLER for their kind suggestions, guidance and support.

I would like to appreciate and thank dear Prof. Dr. Levent BALLİCE, Prof. Dr. Gülden Gökçen AKKURT, Prof. Dr. Müşerref ARDA and my supervisors for the comments, recommendations and taking their precious time as of jury members.

In addition I would like to thank my laboratory group, Esra ALTIOK and Mine ETİ for their suggestions and comments, the undergraduate students who worked with me in this project under my supervision, Tuğçe Zeynep KAYA, Melis TÜZÜN, Islam Rashad Ahmed SENAN, and exchange student from Japan, Soma KITADA.

I have special thanks to my family for all their support, love, encouragement, guidance and comments; especially to my mother Huri KINALI, my father Hikmet KINALI, my brother Özcan KINALI, my sister-in-law Ayşen KINALI and my nephew Atilla KINALI. I am grateful to my mother-in-law Seyhan ÖZ, father-in-law Bahri ÖZ and brother-in-law İsmail Berk ÖZ for all their support, love, encouragement, guidance and comments. Lastly special thanks goes to my beloved wife Pelin KINALI, for her endless support, love, encouragement, guidance and comments.

25 / 08 / 2021

Orhan KINALI

CV

Personel Information:

Name	**Orhan KINALI**
Adress	
Mobile Phone	
E-mail	
Date of Birth	
Driving Licence	
Military Service	

Academic Qualifications:

	Department	School	Date of Graduation	City/Country
Graduate	Chemical Engineering	Ege University	Ongoing (3.71 / 4)	Izmir/Turkey
Undergraduate	Chemical Engineering	Ege University	08.2018 (2.74 / 4)	Izmir/Turkey
High School	Science-Mathematics	Karşıyaka Anadolu Lisesi	06.2013 (82.33 / 100.00)	Izmir/Turkey

Foreign Languages:

	Reading	Writing	Speaking
English	Advanced	Advanced	Advanced
German	Elementary	Elementary	Elementary

Skills:

Computer Applications	Adobe Photoshop CC 2017, Aspentech AspenPlus 2006.5, Autodesk Autocad 2014, COMSOL Multiphysics, ERP Systems, Mathworks MATLAB 2017, Minitab 18, MS Office 2013, NETSIS, POLYMATH Professional, SAP Modules, SolidWorks 2014
Instruments/Devices	FT-IR Spectrometer, Potentiostat/Galvanostat/ZRA, Viscometer, Rheometer, UV/VIS Spectrophotometer
Methods	APQP, PPAP, MSA, SPC, FMEA, FMECA, Lean, Six Sigma, Kaizen, SWOT, Ishikawa (Fishbone), 5 Whys, 8D, What If

Experiences:

Kansai Altan Paint Industry – "Research & Development Center" / İzmir	Process Lab. Project Engineer (03.05.2021 – ongoing)
Zorlu Holding – Meta Nickel Cobalt Mining – "Research & Development Center" / Manisa	R&D Specialist (01.11.2020 – 30.04.2021) R&D Engineer (21.10.2019 – 01.11.2020)

TÜBİTAK-Poland Bilateral Cooperation Program Project – (Project No : 117M023)	Graduate Student Project Researcher (05.10.2018 – 20.10.2019)
PETKİM Petrokimya Holding A.Ş. – "PVC Plant" / İzmir	Intern Chemical Engineer (01.08.2016 – 26.08.2016)
İZSU – "İzmir Water and Sewerage Authority Tahtalı Drinking Water Treatment Plant" / İzmir	Intern Chemical Engineer (03.08.2015 – 28.08.2015)

Certificates:

08/2019	**Energy Technologies Summer School-I, "Fuel-Cell Technologies" – Vestel Savunma Sanayi A.S.** / Niğde Omer Halisdemir Universitesi (Fuel-Cell Technologies, PEM, Exergy, Hydrogen Storage Techniques, Batteries for Automated Vehicles
12/2018	Petrochemical Industry, Its Future and Its Importance for Chemical Engineering – **PETKIM Petrokimya Holding A.Ş.** / Ege Üniversitesi Kimya Mühendisliği
12/2018	Polymers and Polymerization – **Kansai Altan Boya Sanayi A.Ş.** / Ege Universitesi Kimya Mühendisliği
10/2018	Reference 3000 Potentiostat/Galvanostat/ZRA – **Referans Kimya**
05/2018	Analiz Hayatın Her Anında / Günlük Yaşam ve Ileri Analitik Teknikler – **ANT Teknik**
02/2015	4th UKMOP – **IYTE/IZTECH (Izmir Institute of Technology)**
12/2013	Iş Güvenliği Semineri– **ÇASGEM**

Hobbies and Interests:

Hobbies and Interests	3D Modelling/Printers, Chess, E-Sports, Ice Skating, Jogging, Novels, Taekwondo, Table Tennis, Tabletop Games, Tennis.

Club & Association Memberships:

Clubs	Oblivion E-Sports (Founder/Leader) (19.07.2018 – Ongoing)
Memberships	CESS (Chem. Eng. Student Society), EGENSO (Ege University Eng. Society)

Diploma Thesis/Projects:

Master's Degree (August, 2021)	Application of Reverse Electrodialysis Method for Salinity Gradient Energy Generation Supervisor : Prof. Dr. Nalan KABAY, Co-advisor : Dr. Enver GÜLER
Bachelor's Degree (July, 2017)	Preparation and Modelling of Supported Ionic Liquid Membrane (SILM) For The Removal of Heavy Metal Ions From Metal Plating Waste Water Supervisor : Asst. Prof. Dr. Nilay GİZLİ

Presentations:

IEX 2022 Cambridge, UK ORAL	Ion Exchange Conference (IEX) 2022 – A Vision for Future "The Effect of Cell Pair and Flow Velocity in Reverse Electrodialysis (RED) Stack for Generation of Salinity Gradient Energy (SGE)" *Orhan KINALI, Esra ALTIOK, Mine ETI, Soma KITADA, Enver GULER, Nalan KABAY, Marek BRYJAK*
IEX 2022 Cambridge, UK POSTER	Ion Exchange Conference (IEX) 2022 – A Vision for Future "Preparation of Anion Exchange Membranes for Reverse Electrodialysis (RED) Applications" *Mine ETI, Ezgi KARAKOÇ, Orhan KINALI, Enver GULER, Nalan KABAY*

MEMTEK November 18-20, 2019 Istanbul, Turkey POSTER	6th MEMTEK International Symposium on Membrane Technologies and Applications "Effect of Flow Velocity on Performance of Reverse Electrodialysis (RED) System For Harvesting Salinity Gradient Energy" *Orhan KINALI, Mine ETİ, Soma KİTADA, Enver GÜLER, Nalan KABAY, Marek BRYJAK*
MEMTEK November 18-20, 2019 Istanbul, Turkey ORAL	6th MEMTEK International Symposium on Membrane Technologies and Applications "Blue Energy Production by Reverse Electrodialysis (RED) System as a Function of Salinity Gradient" *Orhan KINALI, Mine ETİ, Soma KİTADA, Enver GÜLER, Nalan KABAY, Marek BRYJAK*
ICOEST October 19-23, 2017 Budapest, Hungary POSTER	3rd International Conference on Environmental Science and Technology "Preparation and Modelling of Supported Ionic Liquid Membrane (SILM) For The Removal of Heavy Metal Ions From Metal Plating Waste Water" *Orhan KINALI, Nilay GIZLI*